Physics of Quantum Computation

Dr. Javier Cerrillo

Sommersemester 2016, Technische Universität Berlin

Contents

This lecture presents an introduction to the field of quantum computation and quantum information together with theoretical considerations relevant to their physical implementation. Familiarity with concepts of quantum mechanics is required.

1. Prelude: Quantum teleportation

Let us begin with a simple example that illustrates the counter-intuitive behavior of information in the quantum realm: quantum teleportation. The fundamental message of this protocol is that quantum information can be transferred without the need to send any quantum object, a bizarre statement that sets the scene for the kind of phenomena we would like to explore in this lecture. This example allow us to introduce a methodology that we will follow in the rest of the lecture.

1.1 Description of the protocol

Let us imagine Alice [1] in Auckland wants to send an unknown quantum state $|\psi\rangle = \alpha|0\rangle + \beta|1\rangle$ to her friend Bob in Berlin. She can only communicate with Bob by classical means (phone, internet, postcard...). They do count on an additional resource: they have a qubit each which is in an entangled state of the form

$$|\Phi\rangle = \frac{1}{\sqrt{2}}\left(|0\rangle_A|0\rangle_B + |1\rangle_A|1\rangle_B\right).$$

How can Bob receive the state $|\psi\rangle$?

Exercise 1

Show that $|\Phi\rangle$ cannot be written as a separable state – i.e., in the form $|\zeta\rangle_A|\xi\rangle_B$.

The solution is pretty simple. Alice just needs to measure in which of four possible so-called Bell states her two qubits are, then send her measurement outcome (two bits of information) to Bob, so that he can transform his qubit into state $|\psi\rangle$.

[1] It is a tradition in the quantum information community to give the name Alice (party A) to the first party in a protocol and Bob (party B) to the second party. A C party may be called Charlie or Carol, whereas (mostly in the context of quantum cryptography) a third, ill-intentioned party is usually called Eve (from eavesdropper).

Let us take a closer look at this protocol. First of all, let us define the four Bell states

$$
\begin{aligned}
|\beta_{00}\rangle &\equiv \frac{1}{\sqrt{2}}\left(|00\rangle + |11\rangle\right), \\
|\beta_{01}\rangle &\equiv \frac{1}{\sqrt{2}}\left(|01\rangle + |10\rangle\right), \\
|\beta_{10}\rangle &\equiv \frac{1}{\sqrt{2}}\left(|00\rangle - |11\rangle\right), \\
|\beta_{11}\rangle &\equiv \frac{1}{\sqrt{2}}\left(|01\rangle - |10\rangle\right);
\end{aligned}
$$

and rewrite the three-qubit setting of our problem in terms of these

$$
|\psi\rangle\,|\Phi\rangle = |\psi\rangle\,\frac{1}{\sqrt{2}}\left(|0\rangle_A\,|0\rangle_B + |1\rangle_A\,|1\rangle_B\right) = \frac{1}{2}\sum_{ab}|\beta_{ab}\rangle\,|\psi_{ab}\rangle\,, \tag{1.1}
$$

with

$$
\begin{aligned}
|\psi_{00}\rangle &\equiv \alpha\,|0\rangle + \beta\,|1\rangle\,, \\
|\psi_{01}\rangle &\equiv \alpha\,|1\rangle + \beta\,|0\rangle\,, \\
|\psi_{10}\rangle &\equiv \alpha\,|0\rangle - \beta\,|1\rangle\,, \\
|\psi_{11}\rangle &\equiv \alpha\,|1\rangle - \beta\,|0\rangle\,.
\end{aligned}
$$

Exercise 2
Show that Eq.1.1 holds.

Because the set of Bell states is an orthonormal basis, it is possible to distinguish them with a measurement. The result of the measurement indicates the transformations required on Bob's side in order to recover $|\psi\rangle$:

$$
\begin{aligned}
|\psi\rangle &= |\psi_{00}\rangle\,, \\
|\psi\rangle &= X\,|\psi_{01}\rangle\,, \\
|\psi\rangle &= Z\,|\psi_{10}\rangle\,, \\
|\psi\rangle &= ZX\,|\psi_{11}\rangle\,.
\end{aligned}
$$

In a more compact form $|\psi\rangle = Z^a X^b\,|\psi_{ab}\rangle$, where ab are the two bits of information obtained in the Bell-state measurement.

1.2 Theoretical considerations

The seemingly unphysical consequences of this protocol may raise some concerns in the attentive reader. Here we consider three of them: "isn't this against special relativity?", "why didn't Alice use the phone to tell Bob how to build the state?" and "so what, Alice did send an entangled state to Bob in the first place".

1.2.1 No-communication theorem

The quantum teleportation protocol is often paired with a discussion on the possibility of transferring quantum information faster than light. Indeed, once the Bell measurement has been performed, Bob's state has instantaneously become one of the $|\psi_{ab}\rangle$ states, which have a pretty similiar form to the original state $|\psi\rangle$. Nevertheless, without the knowledge of the bits ab, Bob's state ρ_B is a mixture with probability $\frac{1}{4}$ of each of the possible states, which can be shown to be a state of maximal uncertainty

$$\rho_B = \sum_{ab} \frac{1}{4} |\psi_{ab}\rangle \langle\psi_{ab}| = \frac{1}{2} Id.$$

Furthermore, one can see that the state ρ_B has not varied in the slightest due to Alice's measurement.

Exercise 3

Show that $\sum_{ab} \frac{1}{4} |\psi_{ab}\rangle \langle\psi_{ab}| = \frac{1}{2} Id$ and that $Tr_A |\beta_{ab}\rangle \langle\beta_{ab}| = \frac{1}{2} Id$.

No measurement performed on one partition of a system can be used to communicate information instantly to the other partition, and this is rigorously stated by the no-communication theorem, also known as no-signalling theorem. This is a great relief for quantum physics.

1.2.2 No-cloning theorem

One may wonder why Alice didn't measure the state and just tell Bob about the result so that he could build $|\psi\rangle$ himself. The reason is that Alice cannot just learn the state $|\psi\rangle$ with arbitrary accuracy unless an infinite amount of copies of the same state were available[2]. The no-cloning theorem states, though, that it is impossible to transform an unknown state $|\psi\rangle$ into two perfect copies of itself $|\psi\rangle |\psi\rangle$.

Let us prove the theorem by contradiction. Let us imagine that there exists a unitary operation U that could transform a pair of states $|\psi\rangle |\phi\rangle$ into $|\psi\rangle |\psi\rangle$. In general, for it to be considered a cloning device, the same should happen for another state $|\xi\rangle$ and we could write

$$U |\psi\rangle |\phi\rangle = |\psi\rangle |\psi\rangle ,$$
$$U |\xi\rangle |\phi\rangle = |\xi\rangle |\xi\rangle .$$

Taking the inner product of both equations yields

$$\langle\xi|\psi\rangle = \langle\xi|\psi\rangle^2 ,$$

which implies that this device would only work for a specific state $|\psi\rangle$ and its orthogonal.

[2] See Holevo bounds for a more rigorous study of this aspect.

Exercise 4

Schein. Extend the proof to the case of an open quantum system. For this, consider a third state representing the "environment" and assume the unitary operator acts on the three states. Reference: Nature 299, 802 (1982).

1.2.3 Entanglement swapping

One possible criticism to the quantum teleportation protocol may be that for the entanglement between Alice's and Bob's qubits to exist, they must have interacted at some point in the past, i.e., they must have been in close contact. This is not necessarily true, though. The same result as shown in Eq.1.1 can be used to show that Alice and Bob may share an entangled pair of qubits even if these qubits may have never met before. In essence, the transformation in Eq.1.1 is one where entanglement is transferred between one pair of a tripartite system to another pair. Let us imagine it is Carol that Bob shares an entangled state with, $|\Phi\rangle_{BC} = |\beta_{00}\rangle$. Alice has a pair of entangled qubits, for instance in state $|\beta_{00}\rangle$ as well, and gives one of them to Carol.

In order for Alice and Bob to share an entangled state, all Carol has to do is measure her two qubits in the computational basis. This way, Alice and Bob share an entangled state between two qubits that never met in the past.

Exercise 5

Prove the entanglement swapping protocol.

1.3 Experimental considerations

1.3.1 How to perform a Bell-state measurement

The Bell basis is an orthonormal basis of the two-qubit Hilbert space. All its elements are non-local, entangled states: performing a projective measurement in this basis in the lab may seem impossible. Assuming that only local measurements may be performed in the lab, the possibility exists to unitarily transform the Bell basis into a local basis before measuring. This transformation must have the form

$$U = \sum_{ab} |ab\rangle \langle \beta_{ab}| .$$

We will use this excuse to introduce the concept of gate operations and the circuit model of quantum computation. One can see that the above unitary transformation may be split into a Hadamard gate and a controlled-NOT or CNOT gate. A Hadamard gate is a single-qubit gate that performs the unitary transformation

$$H = |+\rangle \langle 0| + |-\rangle \langle 1| ,$$

where we have defined the eigenstate of the X Pauli matrix as

$$|+\rangle = \frac{1}{\sqrt{2}}\left(|0\rangle + |1\rangle\right),$$
$$|-\rangle = \frac{1}{\sqrt{2}}\left(|0\rangle - |1\rangle\right).$$

A CNOT gate is a two-qubit gate that inverts the value of the target bit when the control bit is true. It follows the truth table 1.1.

Control	Target		Control	Target
0	0		0	0
0	1		0	1
1	0		1	1
1	1		1	0

Table 1.1: Truth table of the CNOT gate.

Exercise 6

Schein. Show that the composition of a CNOT gate and a Hadamard gate on the control bit yields the transformation

$$U = \sum_{ab} |ab\rangle \langle\beta_{ab}| .$$

After application of this transformation, measuring each qubit in the computational basis will yield the outcomes a and b, which are univocally related to the original Bell states. The global effect of the unitary transformation and the local measurement is that of a Bell-state measurement.

1.3.2 Fidelity

Success of an experiment needs to be measured in some form, and the usual figure of merit is the fidelity (resemblance between the expected and measured states)

$$F = Tr\left\{\sqrt{\rho_{expected}^{\frac{1}{2}}\rho_{measured}\rho_{expected}^{\frac{1}{2}}}\right\}.$$

In this specific protocol, assuming pure states

$$F = |_A\langle\psi|\,|\psi\rangle_B| ,$$

with $|\psi\rangle_A$ the state to be teleported by Alice and $|\psi\rangle_B$ the state Bob receives, where an average over possible inputs is usually included. If teleportation follows without error, it is clear $F = 1$. Otherwise $F < 1$. It is important to set up what constitutes the failure of the experiment. A value for the fidelity 0 is actually not necessarily a bad result. It actually is pretty good,

because it may mean that the obtained state is exactly orthogonal to the expected one, so it may be the indication of a swap error in the Bell-state measurement that can be corrected.

In general, in quantum information technologies the real failure is the absence of a quantum advantage. Because it is so difficult to generate quantum technology, it is important that it provides an advantage with respect to the classical analog of the protocol. In this case, the classical analog of quantum teleportation (classical teleportation) is to drop the entanglement resource: attempt to transfer the state by performing a one shot projective measurement on it and transferring the result in two bits of data to Bob so that he can reconstruct the state. In that case, Bob's state is one of either $|+\rangle_n$ or $|-\rangle_n$, the eigenstates of the Pauli matrix σ_n in which the measurement has taken place, and the maximum fidelity that can be obtained with this strategy is $F = 2/3$.

Exercise 7

Schein. Show that the fidelity of the classical scenario is 2/3 by following the considerations in PRL 74, 1259 (1995).

1.3.3 Platforms and variations

Many experimental demonstrations of quantum teleportation have taken place in photonic settings. The polarization degree of freedom of a photon can take one of two values: horizontal or vertical polarization. This can be used to store a qubit. Entangled photons can be obtained by means of a process known as parametric down-conversion, which corresponds to the emission of two photons in a single process.

The longest distance quantum teleportation achieved to date in a photonic setting took place between the islands of La Palma and Tenerife in Spain (Nature, 489(7415), 269, 2012). Other platforms involved nuclear magnetic resonance settings (molecules in solution), optical modes (continuous variable settings), atomic ensembles, trapped atoms, solid state...

Nevertheless, we have just seen that, rather than distance, fidelity is the most relevant figure of merit. Other considerations may involve whether the experiment was deterministic or not. In the case of photons it is usually impossible to distinguish more than two of the Bell states, so that only upon detection is it possible to finalize the protocol. These implementations are known as *probabilistic quantum teleportation*. Some experiments avoid the feed-forward part, i.e. the classical communication of the measurement outcome, so that only upon detection of the first Bell-state is it possible to assume teleportation. This is considered *passive quantum teleportation*.[3]

[3] For a complete review on the subject: Nature Photonics 9, 641, (2015).

2. Circuit model of quantum computation

With quantum teleportation we have seen an example of a quantum protocol for which there exists an algorithmic description in the form of quantum gates. Let us systematize this procedure so that it allows us to define a model for quantum computation, that is, a model that is able to represent any quantum algorithm. Let us begin by learning our first quantum algorithm, then represent it in terms of quantum gates. After this example, we will systematize the approach and analyze it.

2.1 Deutsch-Jozsa algorithm

In the last lecture we got acquainted with a relevant protocol for the quantum information processing (QIP) community: quantum teleportation. It is a protocol that performs something impossible for the classical world (F=1 can never be reached with a classical protocol) and, as such, the only scrutiny that we have to put it under is checking whether it stays within the quantum boundaries ($F > 2/3$). Before we get started with the systematic formulation of quantum computation, let us look at a simple algorithm that can be performed both in the classical and the quantum version, but which shows an advantage in its quantum form. The Deutsch-Jozsa algorithm is the best example of quantum parallelism and the first quantum algorithm ever proposed. For cases where a task can be performed equally well with a classical or a quantum algorithm, the question is whether the quantum version allows us to do it faster or with fewer resources. We will return to this question on a later lecture.

The question posed by the Deutsch-Jozsa algorithm is the following. Given a function $f(x) \in \{0,1\}$ on an n bit input x that is either *constant* (same value for all inputs) or *balanced* (exactly half of times 0 and the other half 1), how fast is it possible to deterministically decide which of the two types of function $f(x)$ belongs to? In the classical case, one needs $2^{n-1}+1$ calls of the function. In the quantum case, only one. This represents an exponential saving!

The quantum version evaluates the function for all possible inputs x by computing it on a superposition state

$$\frac{1}{\sqrt{2^n}} \sum_{x=0}^{2^n-1} |x\rangle ,$$

which is the result of applying the Hadamard gate on n qubits in the state $|0\rangle$.

Exercise 8

Schein. Show that

$$H^{\otimes n}\left|0\right\rangle^{\otimes n} = \frac{1}{\sqrt{2^n}}\sum_{x=0}^{2^n-1}\left|x\right\rangle,$$

where the state $|x\rangle$ corresponds to the n qubit state labeled by the binary expression of integer x. (For instance, the three qubit representation of $|3\rangle$ is $|0\rangle|1\rangle|1\rangle$).

By using the output $f(x)$ as the control of a CNOT gate on an ancilla state $|-\rangle$ one obtains the state

$$\frac{1}{\sqrt{2^{n+1}}}\sum_{x=0}^{2^n-1}\left|x\right\rangle\left[(-1)^{f(x)}\left|0\right\rangle - (-1)^{f(x)}\left|1\right\rangle\right].$$

The final step is to undo the balanced superposition of the $|x\rangle$ states by repeating the application of the Hadamard gate on the first n qubits. This generates the confusing state

$$\frac{1}{2^n\sqrt{2}}\sum_{x=0}^{2^n-1}\sum_{z=0}^{2^n-1}(-1)^{zx+f(x)}\left|z\right\rangle\left[\left|0\right\rangle - \left|1\right\rangle\right],$$

but maybe expressing the phase factor in the following form would help

$$\sum_{x=0}^{2^n-1}(-1)^{zx+f(x)} = \sum_{\mathbf{x}} e^{i\pi[\mathbf{zx}+f(\mathbf{x})]},$$

because it vaguely reminds of a representation of a Kronecker delta. With this idea, it becomes clear that, if $f(x)$ is constant,

$$\frac{1}{2^n}\sum_{\mathbf{x}} e^{i\pi[\mathbf{zx}+f(\mathbf{x})]} = \pm\frac{1}{2^n}\sum_{\mathbf{x}} e^{i\pi\mathbf{zx}} = \begin{cases}\pm 1 & (z=0)\\ 0 & (z\neq 0)\end{cases}$$

which is 1 only for $z=0$. For $f(x)$ balanced and $z=0$

$$\sum_{\mathbf{x}} e^{i\pi[\mathbf{zx}+f(\mathbf{x})]} = \sum_{\mathbf{x}} e^{i\pi f(\mathbf{x})} = 0,$$

because half of the times $e^{i\pi f(\mathbf{x})}$ is $+1$ and half of the times -1. And this is it! Measuring the first n qubits will deterministically yield the state $|0\rangle$ if $f(x)$ is constant and another state if it is balanced.

2.1.1 Examples of circuit representations

Once we have understood the algorithm, let us look at its circuit representation and try to understand all elements therein.

Figure 2.1: Circuit representation of the Deutsch-Jozsa algorithm (Wikipedia).

In the circuit model, qubits are represented by horizontal lines and gates (in the case of quantum computation, they must be unitary operations to preserve reversibility) are represented by boxes. These boxes may have one incoming horizontal line and one outcoming horizontal line (single qubit gates) or more than one (multiple qubit gates). Another possible operation is measurement, which is represented with a "dial" box (last box in the first row of Fig.2.1).

We are already acquainted with the Hadamard gate, since it was an ingredient in turning a Bell-state measurement into a local one (§1.3.1). In this case, we want to apply the Hadamard gate to n qubits. This is represented by a tensorial exponent $H^{\otimes n}$. The symbol right before that gate informs us that that particular horizontal line contains n qubits instead of a single one.

The gate U_f is such that it computes the function $f(x)$ on the first n qubits and uses the outcome to control a NOT gate on the last qubit.

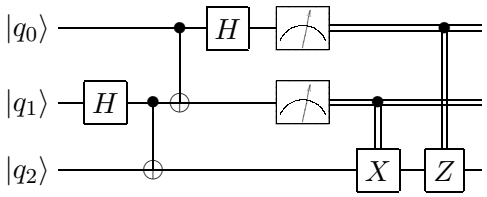

Figure 2.2: Circuit representation of the quantum teleportation protocol (I. Chuang).

Let us look at more elements that may appear in a quantum circuit. Figure 2.2 represents the quantum teleportation protocol. The second and third elements represent a CNOT gate, which we encountered in §1.3.1 as well. The reason for this representation is that the outcome on the second qubit corresponds in essence to a logical XOR operation (represented by $\oplus$) on both qubits. After measurements, we see classical bits are represented by a double line and they can operate on qubits as well. First, with an XOR $\oplus$ operation (corresponding to the application of the Pauli matrix X conditioned on the classical bit). Second, on a conditioned phase gate (Z Pauli matrix).

2.1.2 Experimental implementation

The Deutsch-Jozsa algorithm was not created to solve a specific task of relevance, but to show that quantum computers can solve a task exponentially faster than classical computers.[1] For this reason it has been implemented in a number of platforms. Let us have a look at the case of trapped ions: Nature 421, 48 (2003). There, the simplest version of the Deutsch-Jozsa algorithm (where the function has a single-bit input) was demonstrated. This simplified version

[1] It is important to stress that, although it is exponentially faster than a deterministic classical algorithm, the probabilistic classical algorithm can settle the question very quickly and represents an important competitor to the quantum algorithm.

of the algorithm is sometimes known as the Deutsch algorithm. For this, only two qubits are required and, in this experimental example, they were encoded in two degrees of freedom of a single Ca_{40}^{+} ion: the two lowest lying Fock states of its vibration and two electronic levels. There only exist 4 possible functions, two constant and two balanced, and all 4 of them were implemented in this experiment. It was confirmed that the input state stays $|0\rangle$ for constant functions and becomes $|1\rangle$ for balanced functions.

Although we will look into the trapped-ion platform in more detail below, a trapped ion experiment always contains the steps

1. Loading of the ion into a Paul trap.
2. Laser cooling to the motional ground state (Doppler + sideband cooling).
3. Algorithm performance by shining a train of laser pulses.
4. Measurement.

In order to implement gates on the electronic degrees of freedom, the ion is driven resonantly by laser light for a short time $t = \frac{\theta}{\Omega}$, where Ω is the Rabi frequency, so that the Schrödinger evolution corresponds to the unitary transformation

$$R(\theta, \phi) = \exp\left[i\frac{\theta}{2}\left(e^{i\phi}\sigma^{+} + e^{-i\phi}\sigma^{-}\right)\right],$$

where $\sigma^{+} = |1\rangle\langle 0|$ and $\sigma^{-} = |0\rangle\langle 1|$. The initial phase of the laser ϕ determines whether a rotation on the X or the Y axis is performed (or a desired combination of them).

Exercise 9

Build a Hadamard gate with pulses of the type $R(\theta, \phi)$.

Gates on both the electronic and vibrational degrees of freedom are performed by means of detuned laser driving. By exactly matching the trap frequency with the detuning, the momentum exchange between the light and the atom can be controlled to the extent that the unitary transformation

$$R^{-}(\theta, \phi) = \exp\left[i\frac{\theta}{2}\left(e^{i\phi}\sigma^{+}a + e^{-i\phi}\sigma^{-}a^{\dagger}\right)\right]$$

is performed, where a, $a^{\dagger}$ are the annihilation and creation operators of the vibrational degrees of freedom of the ion respectively. This is an interaction operation between both qubits and we will see below that it is a necessary ingredient to perform two-qubit gates in ion trap experiments.

Exercise 10

Show that $R^{-}(\pi, 0)$ corresponds to a SWAP gate when only considering the lowest two states of the vibrational manifold.

The combination of the two types of pulses allows for the implementation of the 4 different functions in the form of 4 different pulse trains. The pulse trains corresponding to the constant functions always leave the electron on its ground state, whereas pulse trains corresponding to balanced functions leave the electron on the excited level.

2.2 Universal quantum gates

As shown in the experimental implementation of the Deutsch-Jozsa algorithm, it is possible to transform an algorithm into a specific, realizable train of pulses. Let us show that, in principle, any algorithm can be expressed in terms of single- and two-qubit gates.

2.2.1 Two-level unitary gates are universal

This is a problem of linear algebra: given a $d \times d$ unitary matrix U, it is possible to transform it into the identity matrix by multiplying it with enough, judiciously chosen two-level unitary matrices $U_1 U_2 U_3 \ldots$. The conjugate transpose of this set of two-level matrices corresponds to the decomposition of U.

Two level unitary matrices are unitary matrices that act non-trivially only on two vector components. Let us be convinced of this idea by looking at an example with a 3×3 matrix

$$U = \begin{pmatrix} a & d & g \\ b & e & h \\ c & f & i \end{pmatrix}.$$

If $b = 0$ choose

$$U_1 \equiv \begin{pmatrix} 1 & 0 & 0 \\ 0 & 1 & 0 \\ 0 & 0 & 1 \end{pmatrix},$$

and otherwise choose

$$U_1 \equiv \frac{1}{\sqrt{|a|^2 + |b|^2}} \begin{pmatrix} a^* & b^* & 0 \\ b & -a & 0 \\ 0 & 0 & 1 \end{pmatrix}.$$

We have achieved to introduce a 0 in the matrix:

$$U_1 U = \begin{pmatrix} a' & d' & g' \\ 0 & e' & h' \\ c' & f' & i' \end{pmatrix}.$$

For the choice of U_2 we follow a similar procedure. If $c' = 0$ choose

$$U_2 \equiv \begin{pmatrix} a'^* & 0 & 0 \\ 0 & 1 & 0 \\ 0 & 0 & 1 \end{pmatrix},$$

and otherwise

$$U_2 \equiv \frac{1}{\sqrt{|a'|^2 + |c'|^2}} \begin{pmatrix} a'^* & 0 & c'^* \\ 0 & 1 & 0 \\ c' & 0 & -a' \end{pmatrix}.$$

Now we have

$$U_2 U_1 U = \begin{pmatrix} 1 & d" & g" \\ 0 & e" & h" \\ 0 & f" & i" \end{pmatrix} = \begin{pmatrix} 1 & 0 & 0 \\ 0 & e" & h" \\ 0 & f" & i" \end{pmatrix},$$

where $d" = g" = 0$ because unitary matrix only contain normalized vectors as rows/columns. It is clear that this procedure can be continued until the product of unitaries yields the identity.

2.2.2 Single qubit and CNOT gates are universal

Two level unitary gates can be implemented with a succession of CNOT gates and the non-trivial part of the two-level gate, which is a single-qubit gate. We will look at an example again.

Let us imagine a three qubit gate of the form

$$U = \begin{pmatrix} a & 0 & 0 & 0 & 0 & 0 & 0 & b \\ 0 & 1 & 0 & 0 & 0 & 0 & 0 & 0 \\ 0 & 0 & 1 & 0 & 0 & 0 & 0 & 0 \\ 0 & 0 & 0 & 1 & 0 & 0 & 0 & 0 \\ 0 & 0 & 0 & 0 & 1 & 0 & 0 & 0 \\ 0 & 0 & 0 & 0 & 0 & 1 & 0 & 0 \\ 0 & 0 & 0 & 0 & 0 & 0 & 1 & 0 \\ c & 0 & 0 & 0 & 0 & 0 & 0 & d \end{pmatrix}.$$

The non-trivial part of the gate operates between the states $|000\rangle$ and $|111\rangle$ with the gate $\tilde{U} = \begin{pmatrix} a & b \\ c & d \end{pmatrix}$. In order to implement this operation, we need to resort to a so-called Gray code between $|000\rangle$ and $|111\rangle$, which is a sequence of one bit transformations between the initial and the final states

A	B	C
0	0	0
0	0	1
0	1	1
1	1	1

In view of this code, all one has to do is perform one CNOT gate for each transition, the controlled-$\tilde{U}$ gate for the last one and undoing the CNOT gates. For instance, for the transition $|000\rangle \leftrightarrow |001\rangle$ one needs to perform a CNOT gate acting on qubit C conditioned on A and B being 0. The list of the sequence of gates is then

1. CNOT on C, conditioned on A and B being 0,

2. CNOT on B, conditioned on A being 0 and C being 1,
3. controlled-$\tilde{U}$ on A, conditioned on B and C being 1,
4. CNOT on B, conditioned on A being 0 and C being 1,
5. CNOT on C, conditioned on A and B being 0.

This sequence of 5 gates implements U. It is possible to show that the controlled-$\tilde{U}$ gate can be implemented with CNOT and single qubit operations. Therefore, CNOT and single-qubit operations are enough to represent any unitary transformation.

2.2.3 Controlled-U gate

A CNOT gate is sufficient to build any controlled unitary gate. To see this, one can show that there exist unitary gates A, B and C such that $ABC = I$ and $U = e^{i\alpha}AXBXC$. Given the decomposition

$$U = e^{i\alpha} R_z(\beta) R_y(\gamma) R_z(\delta),$$

one may choose $A = R_z(\beta) R_y(\gamma/2)$, $B = R_y(-\gamma/2) R_z(-(\delta+\beta)/2)$ and $C = R_z((\delta-\beta)/2)$. These elements are sufficient to define a controlled-U circuit only with single-qubit gates and CNOT gates.

Exercise 11

Schein: Show that a CNOT gate and arbitrary rotations in the z and y Bloch axes are sufficient to build any controlled U gate.

2.2.4 Discrete sets of universal operations

Exercise 12

Schein: Show that the gate series

$$(THTH)^{n_1} H (THTH)^{n_2} H (THTH)^{n_3}$$

for suitable positive integers n_1, n_2 and n_3 can approximate up to an arbitrarily small error bound any single-qubit unitary U.

CNOT and single qubit gates are universal. Single qubit gates are an infinite set, though. If it is not possible to simulate any possible single qubit gate, it is possible to approximate it by a succession of a discrete set of single qubit gates. Hadamard and $\pi/8$ gates constitute such a set. It is possible to interpret the $\pi/8$ gate as a $\pi/4$ rotation on the z axis up to a global phase, whereas HTH may be interpreted as a $\pi/4$ rotation on the x axis up to a global phase. The combination $THTH$ is a rotation

$$\begin{aligned} R_{\hat{n}}(\theta) = e^{-i\frac{\pi}{8}Z} e^{-i\frac{\pi}{8}X} &= \left(\cos\frac{\pi}{8} - iZ\sin\frac{\pi}{8}\right)\left(\cos\frac{\pi}{8} - iX\sin\frac{\pi}{8}\right) \\ &= \cos^2\frac{\pi}{8} - i\left[(X+Z)\cos\frac{\pi}{8} + Y\sin\frac{\pi}{8}\right]\sin\frac{\pi}{8} \end{aligned}$$

around the non-normalized axis $\vec{n} = \left(\cos\frac{\pi}{8}, \sin\frac{\pi}{8}, \cos\frac{\pi}{8}\right)$ through an angle defined by $\cos\frac{\theta}{2} = \cos^2\frac{\pi}{8}$. This angle is a non-rational multiple of 2π.

3. Trapped ions

In 1995, Peter Zoller and Ignacio Cirac [1] proposed to use electromagnetically trapped ions for the storage and manipulation of quantum information, so that control by localized laser beams would permit the implementation of any logical operation. This was the birth of the first version of a quantum computer that was experimentally realizable. To understand the concepts of this proposal we will analyze the quantum model of a system of trapped ions, we will identify the elements associated with the interface of quantum bits (qubits) and the logic control possibilities offered by the dipolar interaction with the laser. [2]

3.1 Paul traps

The first requirement for the implementation of the Cirac-Zoller proposal is a means to spatially confining individual ions. For this, one often uses strong electromagnetic fields that generate an effective attraction potential, a three-dimensional focalizing force. The electric field that a singly charged calcium ion (Ca^{+}_{40}) experiences corresponds to an acceleration of about $2 \times 10^8 m/s^2$. Although ions can not be trapped only by means of a static electric field, the field of a rapidly oscillating quadrupole geometry,

$$\Phi\left(\vec{x},t\right) = \left(U_0 + V_0 \cos\left(\xi t\right)\right) \frac{x^2 + y^2 - 2z^2}{r_0^2}$$

generates an effective trapping potential under suitably chosen experimental parameters. The fast alternating field prevents the ion from reaching the trap electrodes [3] The entire trajectory of a trapped ion is described by a stable solution of a Mathieu differential equation (Ghosh, 1995). It roughly overlaps a micro-motion of timescale χ and a secular harmonic motion characterized by a lower frequency ν. The three frequencies $\nu_{x,y,z}$ along the three main axes of the trap may be different. Typical individual ion traps are about 1 mm in size with a voltage V_0 several hundred volts and a frequency ξ about 10 MHz, leading to a secular movement frequency ν in the lower MHz range. The linear version of the Paul trap allows for the confinement of several ions, that crystallize in the axis of the trap.

[1] Cirac, J. I., & Zoller, P. , Physical Review Letters 74, 4091 (1995).

[2] Some sections of this part are based on notes by F. Rohde and J. Eschner in Ultracold Gases and Quantum Information, Les Houches 2009 Session XCI, Oxford University Press 2011.

[3] Check `http://youtu.be/XTJznUkAmIY` for a mechanical instantiation of this idea.

3.2 Interaction Hamiltonian

Once the ion is spatially localized, it is possible to control its state with laser light. Laser-ion interaction is usually accounted for by a dipolar term

$$V = -\vec{d} \cdot \vec{E}(t, x),$$

for a dipole $\vec{d}$ of a specific transition between a ground $|g\rangle$ and an excited state $|e\rangle$ and an electric field $\vec{E}$. In the case of a dipole aligned with the coherent field of a laser beam we can use a semiclassical approach so that

$$V = -\hbar \frac{\Omega}{2} \left(|e\rangle \langle g| + |g\rangle \langle e| \right) \left(e^{i(\omega_l t - \vec{k}\vec{x})} + e^{-i(\omega_l t - \vec{k}\vec{x})} \right), \tag{3.1}$$

where Ω is the Rabi frequency ($\Omega = |d|\,|E|$), ω_l is the frequency of the laser, $\vec{k}$ its wavevector and $\vec{x}$ is the operator of the ion position relative to the center of the trap. The total Hamiltonian becomes

$$H = H_0 + V + \Phi\left(\vec{x}\right),$$

with $H_0 = \frac{\hbar\omega_0}{2}\sigma_z$, ω_0 is the frequency associated to the transition between $|g\rangle$ and $|e\rangle$ and $\Phi\left(\vec{x}\right)$ is the time-averaged form of the Paul trap potential. Application of the rotating wave approximation with respect to $\frac{\hbar\omega_l}{2}\sigma_z$

$$V = -\hbar \frac{\Omega}{2} \left(|e\rangle \langle g|\, e^{-ikx} + |g\rangle \langle e|\, e^{ikx} \right). \tag{3.2}$$

Exercise 13

Schein. Show that eq.(3.2) holds in the rotating wave approximation. For this, express the total Hamiltonian H in the interaction picture with respect to $\frac{\hbar\omega_l}{2}\sigma_z$ and average out fast-rotating terms, assuming $\omega_l \simeq \omega_0$. Undo the interaction picture for the remaining terms.

To first approximation $\Phi\left(\vec{x}\right)$ is a harmonic potential in the trap axis x (let's just consider one dimension for simplicity) and can be approximated by

$$\Phi\left(x\right) \simeq \hbar\nu b^\dagger b,$$

with b and $b^\dagger$ annihilation and creation operators, $x = \sqrt{\frac{\hbar}{2m\nu}}\left(b + b^\dagger\right)$. It is useful to introduce the definition of the Lamb-Dicke parameter η

$$\eta \equiv k x_0,$$

with $x_0 = \sqrt{\frac{\hbar}{2m\nu}}$ the extension of the wave function of the ground state. The Lamb-Dicke parameter has a very straightforward interpretation, since it can also be expressed as the square root of the ratio of the recoil energy associated with the process of absorption or emission of a photon and the energy of the photon

$$\eta = \sqrt{\frac{E_{rec}}{E_{ph}}},$$

with $E_{rec} \equiv \frac{(\hbar k)^2}{2m}$ and $E_{ph} \equiv \hbar\nu$. For photons in the optical range, the recoil energy is usually much lower than the photon energy. Alternatively, the photon wavelength is much greater than the extent of ground state ion vibration. Following any of the two interpretations, the Lamb-Dicke parameter in this regime is very small and it can be used as a perturbation parameter which defines the Lamb-Dicke expansion

$$e^{ikx} = e^{i\eta(b+b^\dagger)} = 1 + i\eta(b+b^\dagger) - \eta^2(b+b^\dagger)^2 + \dots$$

and the linearized interaction takes the form

$$V_{lin} = \hbar\frac{\Omega}{2}\left(|e\rangle\langle g| + |g\rangle\langle e|\right) + i\hbar\frac{\Omega}{2}\eta\left(|e\rangle\langle g| - |g\rangle\langle e|\right)\left(b+b^\dagger\right).$$

Three parts can be recognized in this expression, corresponding to three relevant processes hereinbelow. The carrier wave interaction

$$V_{car} = \hbar\frac{\Omega}{2}\left(|e\rangle\langle g| + |g\rangle\langle e|\right),$$

which modifies the internal state of the ion without affecting the vibrational state; red sideband interaction (RSB)

$$V_{RSB} = i\hbar\frac{\Omega}{2}\eta\left(|e\rangle\langle g|\, b - |g\rangle\langle e|\, b^\dagger\right),$$

which excites the internal state of the ion while reducing the vibrations by one photon (and vice versa) state, and the blue sideband interaction (BSB)

$$V_{BSB} = i\hbar\frac{\Omega}{2}\eta\left(|e\rangle\langle g|\, b^\dagger - |g\rangle\langle e|\, b\right),$$

that excites both the internal and the vibrational states.

3.3 Laser cooling techniques

The initial preparation of the ground vibrational state is usually carried out by using laser cooling techniques. In this case, the light-matter interaction is used to extract energy from the vibrational modes of the ion. Let's consider three types of techniques.

3.3.1 Doppler cooling

For very hot ions quantum effects are irrelevant and classical arguments are sufficient to design an effective cooling mechanism. An ion that scatters light from a beam is subjected to a mechanical force in the beam direction. To achieve that this force is always directed away from the ion's displacement (so that it has decelerating power) light must be detuned slightly below the frequency ω_0 (red detuned). Thus, the ion enters into resonance with the light only if it moves towards the source. A red-detuned beam in all spatial directions slows the ion to a velocity below which it does not scatter light. This speed is proportional to the amplitude γ of the absorption line of the chosen electronic transition. For this mechanism to be efficient it is necessary that several scattering events take place within a period of the harmonic trap $\frac{1}{\nu}$, ie the rate γ must be greater than the ν vibration frequency.

3.3.2 Sideband cooling

This mechanism is used after Doppler cooling to reach the ground state of the ions and involves applying a continuous sideband red-shifted beam (3.4), that is, laser light detuned by $\Delta \equiv \omega_l - \omega_0 = -\nu$. Thus, an ion in the state $|g, n\rangle$ is preferentially excited to the state $|e, n-1\rangle$. As the emission process does not change the ion vibrational state in average, the most likely state after emission is $|g, n-1\rangle$. The constant repetition of this cycle due to the continuous beam ends up bringing the ion to the ground state $|g, 0\rangle$.

In order to use this technique it is required that the electronic transition is fine enough so that the vibrational sidebands can identified, ie, the spacing between bands ν must be greater than the amplitude γ transition. This is the opposite regime to the one required in the method of Doppler cooling and therefore different electronic transitions must be used in each case.

3.3.3 Cooling by electromagnetically induced transparency

Finally we consider the influence of the use of dark states and Fano resonances in cooling efficiency. For that we consider an additional ground electronic level and use a Raman setup to illuminate the double transition. This extension allows for the decoupling of the carrier wave transition from the red and blue sideband transitions.

Let's define the lambda system consisting of the ground state $|\downarrow\rangle$ the metastable state $|\uparrow\rangle$ and excited state $|e\rangle$ with dissipation rate γ. The lowest levels are coupled to the excited level by two lasers propagating in opposite directions in Raman configuration (detuned equally to the excited state by Δ). For simplicity, let us consider both provide the same Lamb-Dicke parameter η and have the same frequency Rabi Ω. In the first term of the Lamb-Dicke expansion the following dark state appears

$$|-\rangle = \frac{1}{\sqrt{2}} \left(|\uparrow\rangle - |\downarrow\rangle \right).$$

In the interaction picture with respect to both laser frequencies, the zeroth order Hamiltonian in the Lamb-Dicke expansion is

$$H_{EIT}^{(0)} = \hbar\Delta \left|e\right\rangle \left\langle e\right| + \hbar\nu b^\dagger b + \hbar\frac{\Omega}{2} \left(\left|e\right\rangle \left\langle\uparrow\right| + \left|e\right\rangle \left\langle\downarrow\right| + h.c. \right).$$

In terms of the dark state and the orthonormal state $|+\rangle = \frac{1}{\sqrt{2}} \left(|\uparrow\rangle + |\downarrow\rangle \right)$, the decoupling of $|-\rangle$ from the rest of the system becomes evident:

$$H_{EIT}^{(0)} = \hbar\Delta \left|e\right\rangle \left\langle e\right| + \hbar\nu b^\dagger b + \hbar\frac{\Omega}{\sqrt{2}} \left(\left|e\right\rangle \left\langle +\right| + h.c. \right).$$

Since $|e\rangle$ decays both to $|-\rangle$ and $|-\rangle$ but the excitations in $|+\rangle$ are pumped out at a rate Ω it is clear that the steady state to zeroth order in η is $|-\rangle$.

The dark state $|-\rangle$ is coupled to the excited state by the first order Hamiltonian

$$H_{EIT}^{(1)} = \hbar\frac{\Omega}{\sqrt{2}}\eta \left(i \left|e\right\rangle \left\langle -\right| + h.c. \right) (b + b^\dagger).$$

This coupling comprises both the red and the blue sideband. Analogously to the method of sideband cooling it is now a matter of trying to promote the red sideband through proper choice of detuning. However, in this scheme the state $|e\rangle$ is coupled to the state $|+\rangle$, so it helps to first diagonalize the Hamiltonian $H_{EIT}^{(0)}$ into the dressed (diagonalized) states

$$|D_1\rangle = \cos\theta\,|e\rangle + \sin\theta\,|+\rangle\,,$$
$$|D_2\rangle = \sin\theta\,|e\rangle - \cos\theta\,|+\rangle\,;$$

where the parameter θ is defined by

$$\tan\theta = \frac{\Delta + \sqrt{\Delta^2+\Omega^2}}{\Omega}.$$

The energy eigenvalues are

$$\epsilon_{1,2} = \frac{\Delta \pm \sqrt{\Delta^2+\Omega^2}}{2}.$$

For realistic values of Ω the dressed state in a greater overlap with $|e\rangle$ is $|D_1\rangle$. Therefore, the condition that makes for the most efficient scheme is $\epsilon_1 = -\nu$, which translates into setting the values of detuning and laser intensity such that

$$\Omega^2 = 4\nu(\nu - \Delta).$$

3.3.4 Fano resonance

Another way of using the interference of quantum states for the cooling process control is the possibility to decouple certain electronic states from dissipation.

Consider the single excitation manifold including the electronic states and the photon (not phonon) environment. We refer to $|e,0\rangle$ as the state corresponding to the excited ion and no photon in the environment. This state decays after a time γ^{-1} into one of the continua $|+,1\rangle$ or $|-,1\rangle$, which correspond to the electronic state in one of the ground states and a photon in one of the infinite modes of the electromagnetic bath.

The Hamiltonian $H_{k'}$ of the subspace $\{|e,0\rangle, \{|+,1\rangle\}, \{|-,1\rangle\}\}$ can be diagonalized by the continuum $\{|k'\rangle\}$. Through the laser driving present in the zeroth order Hamiltonian, $|+,0\rangle$ also couples to the continuum $\{|k'\rangle\}$, thus defining a new continuum $\{|k\rangle\}$. Let's see how the excited state overlaps with continuum $\{|k\rangle\}$ that diagonalizes the Hamiltonian H_k for the subspace $\{|+,0\rangle, \{|k'\rangle\}\}$. This Hamiltonian contains $H_{k'}$, the coupling between $|+,0\rangle$ and $|e,0\rangle$ and the energy term $\hbar\omega_+ |+,0\rangle\langle+,0|$. So it is satisfied

$$H_k\,|k\rangle = \left[H_{k'} + \hbar\omega_+\,|+,0\rangle\langle+,0| + \hbar\frac{\Omega_A}{\sqrt{2}}\sigma_x^{(+,e)}\right]|k\rangle = \hbar k\,|k\rangle\,.$$

Projection on $|+\rangle$ (we drop the 0 photon index) produces

$$\omega_+\,\langle+|k\rangle + \frac{\Omega_A}{\sqrt{2}}\,\langle e|k\rangle = k\,\langle+|k\rangle\,.$$

Now the overlap $\langle e|k\rangle$ can be calculated

$$\langle e|k\rangle = \frac{\sqrt{2}}{\Omega_A}\left(k-\omega_+\right)\langle +|k\rangle\,.$$

This introduces a zero in the coupling between the state $|e,0\rangle$ and the continuum, preventing the system from emitting photons at a specific energy $k=\omega_+$. This is a phenomenon known as Fano resonance and can be exploited to protect certain processes from dissipation.

3.4 Quantum gate operation

Several degrees of freedom of the trapped ion can be used as qubits. One usually distinguishes internal qubits, such as two electronic levels, and external qubits, which refer to the ion vibrational states.

An electronic qubit requires two stable levels that allow laser driving at an intensity such that the Rabi frequency Ω is greater than the decay rate γ. Suitable conditions may be either a ground state and an excited metastable state connected by a forbidden optical transition (*optical qubit*), or two hyperfine sub-levels of the ground state of an ion with a nuclear spin different from zero (*hyperfine qubit*). Both cases can be treated as two-level atomic systems with high accuracy $\{|0\rangle, |1\rangle\}$. An optical qubit transition is operated with a single laser, while a hyperfine qubit requires two lasers highly detuned from an intermediate level in Raman configuration. In the case of optical qubits, lack of hyperfine structure in the electronic level scheme makes levels sensitive to environmental magnetic fields and fluctuations of the laser phase, which are sources of decoherence. However, effective qubits can be constructed of multiple quantum states of ions to form a decoherence-free subspace. For a hyperfine qubit, the effect of laser phase noise is reduced because usually the two fields for Raman transition are derived from the same source, and frequency difference is stabilized with a microwave oscillator. The magnetic field sensitivity can also be reduced significantly by using sub-levels with no magnetic moment, or by applying a static magnetic field in which the levels of qubits have the same differential Zeeman displacement.

External qubits are usually the two lowest levels $|0\rangle$ and $|1\rangle$ of the vibrational mode of lowest energy. In the next section we will discuss the laser cooling methods necessary to get rid of thermal fluctuations that mask the quantum nature of this degree of freedom.

Considering first a single trapped ion, the basis for quantum logic operations –the computational subspace (CS)– is formed by the combination of internal and external qubits, ie by the four states $\{|g,0\rangle, |g,1\rangle, |e,0\rangle, |e,1\rangle\}$. The generalization of computational subspace to the case of various ions is simple: it is the product of its internal space qubits and the selected common mode of vibration.

Different interaction Hamiltonians induce different unitary dynamics in the CS. Depending on the frequency detuning of the laser beam (ω_l) with respect to the system frequency (ω_0) it is possible to select via rotating wave approximation one of the interaction terms V_{car}, V_{RSB}

or V_{BSB}. The relevant unitary dynamics are described by

$$U_C(t) = \exp\left[-i\frac{\Omega t}{2}\left(|e\rangle\langle g| + |g\rangle\langle e|\right)\right], \tag{3.3}$$

$$U_-(t) = \exp\left[\frac{\eta\Omega t}{2}\left(|e\rangle\langle g|\, b - |g\rangle\langle e|\, b^\dagger\right)\right], \tag{3.4}$$

$$U_+(t) = \exp\left[\frac{\eta\Omega t}{2}\left(|e\rangle\langle g|\, b^\dagger - |g\rangle\langle e|\, b\right)\right]. \tag{3.5}$$

By defining $\theta \equiv \Omega t$ ($\theta \equiv \eta\Omega t$ for the sidebands) as the angle of rotation of a pulse of duration t and including the inital laser phase ϕ, we may reinterpret the pulsed effect as the rotations that we encountered in §2.1.2

$$R(\theta,\phi) = \exp\left[-i\frac{\theta}{2}\left(|e\rangle\langle g|\, e^{i\phi} + |g\rangle\langle e|\, e^{-i\phi}\right)\right], \tag{3.6}$$

$$R^-(\theta,\phi) = \exp\left[\frac{\theta}{2}\left(|e\rangle\langle g|\, be^{i\phi} - |g\rangle\langle e|\, b^\dagger e^{-i\phi}\right)\right], \tag{3.7}$$

$$R^+(\theta,\phi) = \exp\left[\frac{\theta}{2}\left(|e\rangle\langle g|\, b^\dagger e^{i\phi} - |g\rangle\langle e|\, be^{-i\phi}\right)\right]. \tag{3.8}$$

Choosing the proper angle is possible to transform the state of the CS by successive application of pulses. For example, using the notation $R_+(\theta,\phi)$,

$$|g,0\rangle \xrightarrow{R^+\left(\frac{\pi}{2},0\right)} \frac{1}{\sqrt{2}}\left(|g,0\rangle + |e,1\rangle\right) \xrightarrow{R^+\left(\frac{\pi}{2},0\right)} |e,1\rangle$$
$$|e,1\rangle \xrightarrow{R^+\left(\frac{\pi}{2},0\right)} \frac{1}{\sqrt{2}}\left(-|g,0\rangle + |e,1\rangle\right) \xrightarrow{R^+\left(\frac{\pi}{2},0\right)} -|g,0\rangle.$$

The key to building quantum gates with trapped ions is the common mode of vibration. Excitation of the sideband of an ion modifies the state of movement of the chain and has an effect on the subsequent sideband interaction of all other ions, thereby providing the necessary ion-ion coupling. Because of the strong Coulomb coupling between the ions, the vibrational modes are separated and are spectrally distinguishable in energy, so that it is possible to accurately tune the laser to the specific sidebands. The lowest frequency modeν, the center of mass, is separated from the adjacent mode, stretch mode, by $\left(\sqrt{3}-1\right)\nu$.

Let us illustrate the role of the vibrational modes basic role by considering the entanglement of two trapped ions. Two laser pulses individually address each of the two ions. The pulses are defined analogously to equations (3.6-3.8) with additional superscript (1) or (2) indicating the addressed ion. Thus, from the ground state $|g,g,0\rangle$, the following sequence of pulses creates the first Bell state $\left(|e,e\rangle + |g,g\rangle\right)/\sqrt{2}$ and leaves the motional qubit in the ground state:

$$|g,g,0\rangle \xrightarrow{R^{+(1)}\left(\frac{\pi}{2},0\right)} \frac{1}{\sqrt{2}}\left(|g,g,0\rangle + |e,g,1\rangle\right) \xrightarrow{R^{-(2)}(\pi,0)} \frac{1}{\sqrt{2}}\left(|g,g,0\rangle + |e,e,0\rangle\right).$$

3.4.1 Cirac-Zoller gate

There exist several specific protocols for two-qubit gates. The Cirac-Zoller phase gate proposal requires an additional electronic state in the second ion as an auxiliary state $|aux\rangle$. The implementation consists of chaining the three pulses

$$R^{-(1)}(\pi,0)\,R^{-(2),aux}(2\pi,0)\,R^{-(1)}(\pi,0)\,,$$

where $R^{-(2),aux}(2\pi,0)$ refers to a gate involving electronic states $|g\rangle$ and $|aux\rangle$ instead of the usual $|g\rangle$ and $|e\rangle$. We can analyze the effect of each of the pulses with the truth table

Initial state	$R^{-(1)}(\pi,0)$	$R^{-(2),aux}(2\pi,0)$	$R^{-(1)}(\pi,0)$
$\|g,g,0\rangle$	$\|g,g,0\rangle$	$\|g,g,0\rangle$	$\|g,g,0\rangle$
$\|g,e,0\rangle$	$\|g,e,0\rangle$	$\|g,e,0\rangle$	$\|g,e,0\rangle$
$\|e,g,0\rangle$	$-\|g,g,1\rangle$	$\|g,g,1\rangle$	$\|e,g,0\rangle$
$\|e,e,0\rangle$	$-\|g,e,1\rangle$	$-\|g,e,1\rangle$	$-\|e,e,0\rangle$

As we see the overall effect of the pulse sequence is the addition of a phase only if the initial state is $|e,e\rangle$. From the perspective of the X basis

$$|\pm\rangle = \frac{1}{\sqrt{2}}\left(|g\rangle \pm |e\rangle\right),$$

this can be interpreted as a CNOT gate! The set formed by the single-ion gates (3.6-3.8) and the proposed Cirac-Zoller gate constitute a universal set, turning trapped ions into a quantum computer.

3.4.2 Mølmer-Sørensen gate

The Mølmer-Sørensen gate constitutes a successful attempt to relax the requirement for ground-state cooling of the vibrational degrees of freedom and of individual addressing of the ions. Considering a setting for two ions, two laser beams, one detuned close to the red sideband and the other one detuned close to the blue sideband, are directed to both ions. In this situation virtual, two-photon transitions are the most likely, so that the state of both ions is simultaneously and coherently modified. By choosing the interaction time appropriately the following truth table is satisfied

Initial state	Final state
$\|g,g\rangle$	$\frac{1}{\sqrt{2}}\left(\|g,g\rangle + i\,\|e,e\rangle\right)$
$\|g,e\rangle$	$\frac{1}{\sqrt{2}}\left(\|g,e\rangle + i\,\|e,g\rangle\right)$
$\|e,g\rangle$	$\frac{1}{\sqrt{2}}\left(\|e,g\rangle + i\,\|g,e\rangle\right)$
$\|e,e\rangle$	$\frac{1}{\sqrt{2}}\left(\|e,e\rangle + i\,\|g,g\rangle\right)$

From the perspective of basis $|\pm\rangle = \frac{1}{\sqrt{2}}\left(|g\rangle \pm |e\rangle\right)$, this becomes

Initial state	Final state
$\|++\rangle$	$\|++\rangle$
$\|+-\rangle$	$i\,\|+-\rangle$
$\|-+\rangle$	$i\,\|-+\rangle$
$\|--\rangle$	$\|--\rangle$

up to a phase factor $\frac{1+i}{\sqrt{2}}$. This is a conditional phase gate up to single-qubit phase shifts. This once more reveals the connection between entangling gates and non-trivial two-qubit gates, as we saw in §1.3.1. There exist a number of other proposals that attempt to circumvent other experimental limitations of ion-trap setups.

3.4.3 Composite gates

For efficiency reasons it is sometimes useful to use a different structure for the experimental implementation of certain gates. This can solve problems like imperfect individual addressing of ions, populating Fock states out of the computational basis or time constraints. Let us have a look at some examples.

In situations where single ions cannot be addressed individually with sufficient accuracy, single ion gates can be split into several terms so that the global effect in neighboring ions is less strong than the original gate. For instance

$$R(\pi,0) = R\left(\frac{\pi}{2},\pi\right) R_z(\pi)\, R\left(\frac{\pi}{2},0\right),$$

where $R_z(\pi) = e^{-i\frac{\pi}{2}\sigma_z}$. One way to implement a $R_z(\pi)$ gate is by applying an intense but far detuned laser, so that an AC-Stark shift takes place. Assuming that a neighboring ion is inadvertently affected by the same beam with an intensity factor ϵ, the gate applied there is

$$R\left(\epsilon\frac{\pi}{2},\pi\right) R_z\left(\epsilon^2\pi\right) R\left(\epsilon\frac{\pi}{2},0\right),$$

which is closer to unity than the effect of the non-composite gate effect $R(\epsilon\pi,0)$.

An alternative to the Cirac-Zoller gate that does not involve an auxiliary electronic state is

$$R^{-,aux}(2\pi,0) = R^{+}\left(\frac{\pi}{2},\frac{\pi}{2}\right) R^{+}\left(\frac{\pi}{\sqrt{2}},0\right) R^{+}\left(\frac{\pi}{2},\frac{\pi}{2}\right) R^{+}\left(\frac{\pi}{\sqrt{2}},0\right),$$

It is convenient to think of this gate in terms of the two levels that it involves for each input. The state $|e,0\rangle$ is not affected, whereas both $|g,0\rangle$ and $|e,1\rangle$ experience a 2π rotation within that cycle and $|g,1\rangle$ with $|e,2\rangle$, which is a state out of the computational subspace.

Similarly, a SWAP gate between a motional and electronic qubit can be implemented with

$$R^{+}\left(\frac{\pi}{\sqrt{2}},0\right) R^{+}\left(\frac{2\pi}{\sqrt{2}},\arccos\left[\cot^2\frac{\pi}{\sqrt{2}}\right]\right) R^{+}\left(\frac{\pi}{\sqrt{2}},0\right).$$

4. Quantum algorithms

The promises of quantum computation concretized after Shor demonstrated in 1994 that large numbers could be factorized efficiently. Given the fact that widely extended cryptographic tools are based on the difficulty to factorize large numbers with classical computers, this discovery quickly gathered global attention. In addition to Shor's algorithm, Grover's search algorithm was shown to provide a quadratic improvement of exponentially complex problems, and also establishes the limitations of quantum computation. The following sections provide a pragmatic overview of the most important aspects of these algorithms.

4.1 Shor's factorization algorithm

A crucial element in Shor's algorithm is the possibility to perform a quantum Fourier transform efficiently. Let us quickly review the necessary elements to perform it.

4.1.1 Quantum Fourier transform

For a complex function x_j defined on a discrete domain $j \in \{0, \ldots, 2^n - 1\}$, we define its Fourier transform y_k as

$$y_k = \frac{1}{\sqrt{2^n}} \sum_{j=1}^{2^n-1} e^{i\frac{2\pi}{2^n}jk} x_j \tag{4.1}$$

and its quantum version as

$$\sum_{j=1}^{2^n-1} x_j \left|j\right\rangle \rightarrow \sum_{k=1}^{2^n-1} y_k \left|k\right\rangle, \tag{4.2}$$

where y_k is as defined in Eq.(4.1). By using the n-bit representation $j_1 j_2 \ldots j_n \equiv j_1 2^{n-1} + j_2 2^{n-2} + \cdots + j_n 2^0 = j$ and the fractional representation $0.j_l j_{l+1} \ldots j_m \equiv j_l/2 + j_{l+1}/4 + \cdots + j_m/2^{m-l+1}$, it is possible to reduce the quantum Fourier transform Eq.(4.2) to the transformation

$$\left|j\right\rangle \rightarrow \frac{1}{2^{n/2}} \left(\left|0\right\rangle + e^{i2\pi 0.j_n} \left|1\right\rangle\right) \left(\left|0\right\rangle + e^{i2\pi 0.j_{n-1}j_n} \left|1\right\rangle\right) \ldots \left(\left|0\right\rangle + e^{i2\pi 0.j_1 j_2 \ldots j_n} \left|1\right\rangle\right), \tag{4.3}$$

where the product contains n elements, corresponding each to a single of the n qubits required to represent indices j or k. This unitary transformation can be implemented as shown by the circuit in figure 4.1. Starting with an arbitrary n-qubit computational eigenstate, action

with a Hadamard gate on the first qubit $|j_1\rangle$ produces the superposition $\frac{1}{\sqrt{2}}\left(|0\rangle + e^{i2\pi 0.j_1}|1\rangle\right)$. Accumulation of phase on the state $|1\rangle$ of the first qubit conditioned on the states of the remaining qubits by the $C(R_k)$ gates produces the superposition $\frac{1}{\sqrt{2}}\left(|0\rangle + e^{i2\pi 0.j_1 j_2 \ldots j_n}|1\rangle\right)$. Iterative application of this module on the remaining qubits and a final SWAP operation finally amounts to the transformation Eq.(4.3).

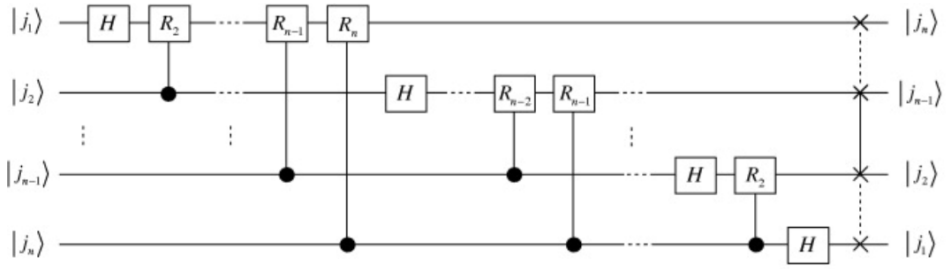

Figure 4.1: Circuit for the Quantum Fourier Transform

Exercise 14

Schein: Explain the steps involved in the quantum Fourier transform and give a definition for the required gates R_n.

4.1.2 Phase estimation

Building up on the quantum Fourier transform, one can devise a method to estimate a specific eigenvalue of a unitary transformation U. Let us define the phase ϕ corresponding to the eigenvalue $u_\phi \equiv e^{i\phi}$ associated to the eigenvector $|u_\phi\rangle$ of interest. Figure (4.2) shows the corresponding quantum circuit.

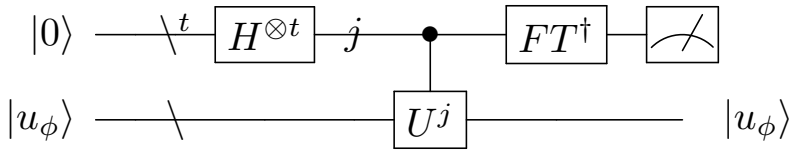

Figure 4.2: Phase estimation protocol

By performing controlled-U^j operations on the target, which encodes the eigenvector $|u_\phi\rangle$, one is performing a phase gate on the control qubits. For t the number of control qubits, one obtains the Fourier transform of the state $\left|\tilde{\phi}\right\rangle$, where $\tilde{\phi}$ is the t-bit approximation of the phase ϕ. Application of the inverse Fourier transform and measurement on the computational basis yields an approximation of the basis.

4.1.3 Order finding

Phase estimation can in turn be used to obtain the *order* r of an integer x modulo N, which is the lowest integer r such that the remainder of the division of N by x^r is 1. In the language of modular arithmetic, the order of x is r such that $x^r = 1 \,(\mod N)$. By defining the unitary

$$U\left|y\right\rangle = \left|xy \,(\mod N)\right\rangle$$

one can obtain the order of x from the eigenstate

$$\left|u_s\right\rangle \equiv \frac{1}{\sqrt{r}} \sum_{k=0}^{r-1} \exp\left[\frac{-i2\pi sk}{r}\right] \left|x^k \,(\mod N)\right\rangle .$$

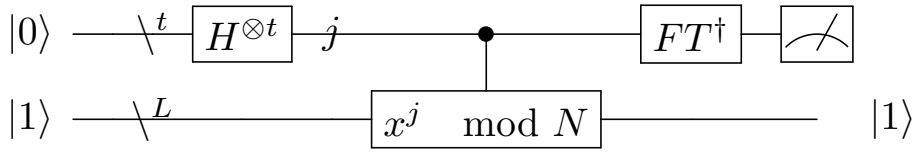

Figure 4.3: Order finding protocol

Notice that $\left|1\right\rangle = \frac{1}{\sqrt{r}} \sum_s^{r-1} \left|u_s\right\rangle$. By preparing the correct circuit, one obtains an estimation of $\frac{s}{r}$. Continued fraction representation provides r, which in turn is related through a classical algorithm to the factorization of N.

4.2 Grover's search algorithm

This constitutes a second class of useful algorithms that provides a considerable speedup with respect to their classical counterparts, albeit "just" a quadratic speedup. The common example to illustrate this algorithm is called the *traveling salesman* problem, and involves finding the shortest of N routes connecting a number of cities. Classically, it takes $O\left(N\right)$ operations to find the solution. Quantum computation offers the possibility to solve the problem with just $O\left(\sqrt{N}\right)$ operations. It turns out that many problems can be expressed in terms of a search. Let's take the the problem of factorizing a large number m, for instance, which is addressed by Shor's algorithm. The most naive (and inefficient) approach is to check all numbers one by one between 2 and $m^{1/2}$ to see if they are factors of m. Classically, this would require $O\left(m^{1/2}\right)$ operations, whereas the quantum search algorithm would speed this up to $O\left(m^{1/4}\right)$. Although this is not a useful case (even classical algorithms exist that do much better), it comes to show that a quadratic improvement is always possible whenever a classical algorithm can be expressed in terms of a search.

4.2.1 Procedure

Let us reformulate the problem that we want to address in terms of a space of $N = 2^n$ elements, so that elements can be indexed with n bits. Let us assume a given problem is solved by M of these elements (in other words, M elements satisfy the conditions set by the problem). This can be encoded in a function $f(x)$ which takes n-bit indices x and outputs 1 if element x is a solution to the problem and 0 if it isn't. We encountered these n-bit to 1-bit functions in the Deutsch-Jozsa algorithm. Just as we did there, let us assume we are provided with a quantum circuit O that we call *oracle*, which performs the following transformation on $n+1$ qubits

$$|x\rangle |q\rangle \xrightarrow{O} |x\rangle |q \oplus f(x)\rangle .$$

This gate is analogous to the gate U_f of Fig.(2.1). If we choose $|q\rangle = \frac{1}{\sqrt{2}}(|0\rangle - |1\rangle)$, let us recall that the effect of O is

$$|x\rangle \frac{1}{\sqrt{2}}(|0\rangle - |1\rangle) \xrightarrow{O} (-1)^{f(x)} |x\rangle \frac{1}{\sqrt{2}}(|0\rangle - |1\rangle),$$

that is, a phase -1 is gained only if x is a solution of the problem.

The algorithm consists in the repeated application of a module known as *Grover iteration* or *Grover operator*, denoted G, on the input $|\psi\rangle = \frac{1}{\sqrt{2^n}} \sum_{x=0}^{2^n-1} |x\rangle$. This module works, just as O, on $n+1$ qubits and has 4 steps:

$$G = H^{\otimes n} (2 |0\rangle \langle 0| - I) H^{\otimes n} O \tag{4.4}$$

1. application of the oracle O,
2. application of the Hadamard transform on the first n qubits $H^{\otimes n}$,
3. application of the unitary transformation $2 |0\rangle \langle 0| - I$ on the first n qubits (addition of a -1 phase to all computational states $|x\rangle$ except $|0\rangle$),
4. application of the Hadamard transform on the first n qubits $H^{\otimes n}$.

Note that only O requires the extra qubit, so we may drop it and focus on the first n qubits for the rest of the discussion.

Exercise 15

Schein: Show that, for $|\psi\rangle = \frac{1}{\sqrt{2^n}} \sum_{x=0}^{2^n-1} |x\rangle$

$$H^{\otimes n} (2 |0\rangle \langle 0| - I) H^{\otimes n} = 2 |\psi\rangle \langle \psi| - I$$

and that

$$(2 |\psi\rangle \langle \psi| - I) \sum_k c_k |k\rangle = \sum_k [2 \langle c\rangle - c_k] |k\rangle ,$$

with $\langle c\rangle = \frac{1}{2^n} \sum_k c_k$.

4.2.2 Interpretation

Let us define the equal superposition state of the M indices that satisfy the search problem

$$|\beta\rangle \equiv \frac{1}{\sqrt{M}} \sum_{x'} |x'\rangle ,$$

where x' precisely indicates "solution" states (such that $f(x') = 1$). Analogously, let us define the equal superposition of all those states that are *not* a solution to the problem

$$|\alpha\rangle \equiv \frac{1}{\sqrt{N-M}} \sum_{x"} |x"\rangle ,$$

where $x"$ is now a sum over indices such that $f(x") = 0$. It becomes clear that the full superposition state can be expressed as a superposition of them

$$|\psi\rangle = \sqrt{\frac{N-M}{N}} |\alpha\rangle + \sqrt{\frac{M}{N}} |\beta\rangle \equiv \cos\frac{\theta}{2} |\alpha\rangle + \sin\frac{\theta}{2} |\beta\rangle .$$

Now, within this subspace, $G = (2|\psi\rangle\langle\psi| - I)O$ operates as a composition of a reflection about $|\alpha\rangle$ performed by O and a reflection about $|\psi\rangle$ performed by $(2|\psi\rangle\langle\psi| - I)$. In particular, one can show that

$$G^k |\psi\rangle = \cos\left(\frac{2k+1}{2}\theta\right) |\alpha\rangle + \sin\left(\frac{2k+1}{2}\theta\right) |\beta\rangle .$$

Therefore, repeated application of the Grover operator brings the state closer and closer to the superposition of solutions $|\beta\rangle$ that we are looking for. In particular, in order to get close to $|\beta\rangle$ with probability more than one half, one needs to operate G an amount of times

$$R = CI\left(\frac{\arccos\sqrt{M/N}}{\theta}\right),$$

with $CI(r)$ the closest integer below the real number r. With this result it becomes clear that knowledge of M is required in order to maximize the probability to measure a solution. It is possible to show that this is not the case with the help of the concepts discussed in the next subsection. At any rate, R gives an indication of the quadratic speedup associated to Grover's algorithm. Under the condition that $M \leq \frac{N}{2}$,

$$R \leq CI\left(\frac{\pi}{4\theta}\right) \leq CI\left(\frac{\pi}{4}\sqrt{\frac{N}{M}}\right),$$

so that Grover's algorithm is $O\left(\sqrt{N}\right)$. In particular, it can be demonstrated that not only is that an upper bound but also a lower bound. In this sense, it is impossible to improve search algorithms by means of the implementation of an oracle.

4.2.3 Quantum counting

When the number of possible solutions M is not known, it is possible to derive a reasonable estimate by using the phase estimation procedure. Since G acts as a rotation in the $|\alpha\rangle |\beta\rangle$ plane, it just contains two eigenvalues $e^{\pm i\theta}$. Irrespective of the input state, it is possible to obtain θ and therefore to infer M.

The consequences of this are quite interesting, since it allows to decide whether a specific search problem has a solution or not without checking all exponentially many candidates.

5. Quantum simulations

The high degree of control of quantum systems has a straightforward application that has seen a large surge in the past few years: the possibility to simulate the dynamics otherwise inaccessible quantum systems. In general, classically simulating quantum systems requires exponentially increasing resources with the number of particles, whereas quantum simulation allows for the realization of the same task with usually just a polynomial overhead. Most relevant advances in this field have occurred in cold atom and trapped ion experiments.

One should distinguish between digital quantum simulations (DQS) and analog quantum simulations (AQS). The former represents quantum evolution in a generic platform by means of single and two-qubit gates, therefore remaining very close to the circuit model of quantum computation. The latter is based on a mapping of the quantum system of interest onto the experimental platform, so that the proper evolution of the experimental platform directly represents the dynamics of the quantum system of interest.

5.1 Digital quantum simulation

Representation of the evolution in terms of a polynomially large set of local gates is sometimes possible thanks to the Trotter formula

$$e^{dt(A+B)} \simeq e^{dtA} e^{dtB},$$

for small enough dt. Higher order corrections to this formula are given by the Baker-Campbell-Hausdorff formula. In general, this provides a connection between the evolution of a quantum system whose Hamiltonian has a number of terms of small support (few-particle interactions) and a series of unitary operation. In some sense, we have already seen a deployment of this idea in the ion trap case: the implementation of certain quantum gates by means of the control of the evolution of a quantum system. In order to gain further insight into the flexibility offered by this possibility, let us study in abstract terms the interpretation of the search algorithm as a quantum simulation.

5.1.1 Grover's algorithm as a quantum simulation

Let us postulate a system that is able to implement the Hamiltonian

$$H = |x\rangle \langle x| + |\psi\rangle \langle \psi| ,$$

where $|\psi\rangle$ is a starting state and $|x\rangle$ is a solution to the search. A decomposition $|\psi\rangle = \alpha|x\rangle + \beta|y\rangle$, where $\langle x|y\rangle = 0$, is possible, so that the Hamiltonian in the basis $\{|x\rangle, |y\rangle\}$ takes now the form

$$H = \begin{pmatrix} 1 & 0 \\ 0 & 0 \end{pmatrix} + \begin{pmatrix} \alpha^2 & \alpha\beta \\ \alpha\beta & \beta^2 \end{pmatrix} = I + \alpha(\beta X + \alpha Z),$$

since $\alpha^2 + \beta^2 = 1$. Thus, evolution of the initial state under this Hamiltonian takes the form

$$\exp(-iHt)|\psi\rangle = e^{-it}[\cos(\alpha t)|\psi\rangle - i\sin(\alpha t)(\beta X + \alpha Z)|\psi\rangle]$$

where time is dimensionless or the energy scale of the Hamiltonian is assumed 1. One can show

$$(\beta X + \alpha Z)|\psi\rangle = |x\rangle$$

and therefore the state evolves following

$$|\psi\rangle(t) = \cos(\alpha t)|\psi\rangle - i\sin(\alpha t)|x\rangle$$

By choosing the uniform superposition state as the initial state

---

Exercise 16

Schein: Show that

$$H = |x\rangle\langle\psi| + |\psi\rangle\langle x|$$

reproduces a similar result.

$$|\psi\rangle = \frac{1}{\sqrt{2^n}} \sum_{j=0}^{2^n-1} |j\rangle$$

we have an exact prediction for the time that the Hamiltonian needs to be applied in order to obtain the solution $|x\rangle$ with probability one: $t = \frac{\pi}{2}2^{n/2}$, which indicates the quadratic advantage which is symptomatic of Grover's algorithm. Together with the quantum counting protocol, one can generalize this approach to the case with an unknown number of solutions.

We have a Hamiltonian that is able to reproduce our algorithm. The Trotter decomposition allows us to decompose it into an alternate implementation of very small time-steps dt involving the operations $\exp(-i|x\rangle\langle x|\,dt)$ and $\exp(-i|\psi\rangle\langle\psi|\,dt)$. The effect of one of the cycles

$$U(dt) = \exp(-i|\psi\rangle\langle\psi|\,dt)\exp(-i|x\rangle\langle x|\,dt)$$

can be derived by using the Bloch vector representation

$$|x\rangle\langle x| = \frac{I + \hat{z}\boldsymbol{\sigma}}{2},$$
$$|\psi\rangle\langle\psi| = \frac{I + \hat{\psi}\boldsymbol{\sigma}}{2},$$

with $\hat{z} = (0, 0, 1)$ and $\hat{\psi} = \left(2\alpha\beta, 0, \alpha^2 - \beta^2\right)$. It takes the form

$$U(dt) = \left(\cos^2\frac{dt}{2} - \hat{\psi}\cdot\hat{z}\sin^2\frac{dt}{2}\right) I - i\sin\frac{dt}{2}\left[\left(\hat{\psi}+\hat{z}\right)\cos\frac{dt}{2} - \hat{\psi}\times\hat{z}\sin\frac{dt}{2}\right]\boldsymbol{\sigma}$$

which corresponds to a rotation around the axis

$$\vec{r} = \left(\hat{\psi}+\hat{z}\right)\cos\frac{dt}{2} - \hat{\psi}\times\hat{z}\sin\frac{dt}{2}$$

and an angle

$$\cos\frac{\theta}{2} = \cos^2\frac{dt}{2} - \hat{\psi}\cdot\hat{z}\sin^2\frac{dt}{2} = 1 - \frac{1}{2^{n-1}}\sin^2\frac{dt}{2}.$$

This shows that the choice $dt = \pi$ maximizes the effect of the rotation, so that fewest applications of $U(dt)$ are needed. In that case

$$U(\pi) = \exp\left(-i\left|\psi\right\rangle\left\langle\psi\right|\pi\right)\exp\left(-i\left|x\right\rangle\left\langle x\right|\pi\right) = \left(I - 2\left|\psi\right\rangle\left\langle\psi\right|\right)\left(I - 2\left|x\right\rangle\left\langle x\right|\right)$$

which corresponds identically to the Grover operator defined in the last lecture in Eq.4.4. Because of the properties of qubit algebra and because our objective is to reach the state $|x\rangle$, it turns out to be more efficient to implement the decomposition using long time-steps but, in any rate, we now have a decomposition of the Hamiltonian H in a series of gates that were described in the last lecture. In this sense, we have proposed a digital simulation of Hamiltonian H.

5.1.2 Simulation of general non-local terms

In general, it is always possible to propose a simulation of a given Hamiltonian in terms of two-qubit and single-qubit gates, in a consequence of the discussion in §2.2.2. Nevertheless, it may be more efficient to represent a unitary transformation in terms of non-local Hamiltonian terms. These generally take the form

$$H_n = \bigotimes_{j=1}^{n} \sigma^k_{c(k)}$$

where $c(k) \in \{0, 1, 2, 3\}$ specifies the Pauli matrix and the superindex specifies the qubit upon which it acts. Hamiltonian terms of the form H_n can be viewed as a generalization of a parity operator: the state upon which it acts acquires a global phase depending on whether the amount of qubits in up eigenstates of their corresponding Pauli matrix $\sigma^k_{c(k)}$ is odd or even. With this insight, non-local terms can easily be simulated by transferring the parity to an ancilla qubit, introducing the state-conditioned phase in the ancilla qubit, and returning the acquired phase to the original qubits.

Let us look at an example for better understanding. We consider simulation of the Hamiltonian

$$H = X_1 \otimes Y_2 \otimes Z_3,$$

for which an eigenstate of positive parity is

$$\frac{1}{2}\left(|0\rangle - |1\rangle\right)\left(|0\rangle - i\,|1\rangle\right)|0\rangle\,,$$

and one with negative parity is

$$\frac{1}{2}\left(|0\rangle + |1\rangle\right)\left(|0\rangle + i\,|1\rangle\right)|1\rangle\,.$$

Parity may be accumulated on an ancilla qubit by means of a CNOT gate or modifications thereof by means of single qubit rotations. The ancilla qubit may be operated on with a rotation e^{-iZt} and finally all CNOT gates must be undone. This is represented in Fig.5.1 for our example Hamiltonian.

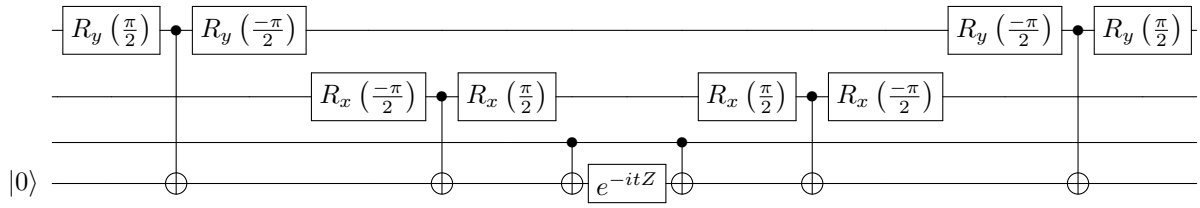

Figure 5.1: Implementation of a non-local Hamiltonian term.

5.1.3 Obtention of molecular energies

The phase estimation algorithm has a clear flavor of quantum simulation. If one is able to prepare an eigenstate of a certain Hamiltonian, it is possible to learn its energy by letting it evolve in time and by extracting the acquired phase. This idea was presented [1] in 2005 together with an iterative version of the phase estimation procedure, so that even with a small number of working qubits, it is possible to repeat the algorithm to increase the accuracy of the obtained phase. The circuit corresponding to this procedure is presented in Fig.5.2 and the definition of V_k is

$$V_k = \left[e^{-i2\pi\phi_{k-1}} V_{k-1}\right]^2,$$

with $V_0 = \exp iH\tau$ and ϕ_{k-1} the phase as known up to iteration $k-1$. The factor $e^{-i2\pi\phi_{k-1}}$ acts as an offset that eliminates the already known bits of accuracy of the phase, and the squared is required to increase the time of the evolution, so that the accumulated phase is double and accuracy can be increased.

[1] Aspuru-Guzik, A., Dutoi, A. D., Love, P. J., & Head-Gordon, M., Science, 309, 1704 (2005).

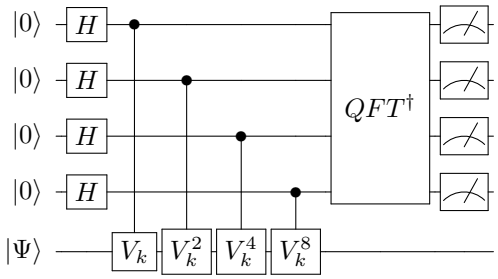

Figure 5.2: Iterative circuit for the obtention of molecular energies.

5.2 Analog quantum simulators

Quantum simulations need not be formulated in terms of quantum circuits. An alternative idea involves a mapping between the Hamiltonians of two different systems: one which is difficult to control and access, and another one which has an controllable experimental implementation. Many instances of this idea have appeared in the last two decades and it is currently the most promising and fastest growing field in quantum computation. Let us review a few examples.

5.2.1 Cold atoms

The possibility to arrange cold neutral atoms in optical lattices allows for the accurate preparation of condensed matter models. A particularly interesting one is the Hubbard model

$$H = -J \sum_{i,j} b_i^\dagger b_j + \frac{1}{2} U \sum_i n_i \left(n_i - 1\right) + \sum_i \mu_i n_i,$$

which can be seen as a lattice of anharmonic, bosonic wells. This is a minimal model for the description of superconducting systems and has been experimentally demonstrated in a cold-atom lattice implementation, where the Mott-insulating (MI) to superfluid (SF) quantum phase transition was demonstrated. Quantum phase transitions are abrupt changes in the ground state of a Hamiltonian as some parameters are changed, so they take place at zero temperature. Assuming no lattice bias μ_i, the two phases are characterized by the two ground states

$$|\Psi_{\mathrm{SF}}\rangle|_{U=0} \propto \left(\sum_{i=1}^{M} b_i^\dagger\right)^N |0\rangle\,,$$
$$|\Psi_{\mathrm{MI}}\rangle|_{J=0} \propto \prod_{i=1}^{M} \left(b_i^\dagger\right)^n |0\rangle\,,$$

where N is the total number of atoms, M is the number of lattice sites and $n = \frac{N}{M}$ is a commensurate filling factor. As the atom-atom repulsion U is increased, atoms tend to

localize in the lattice, whereas for large tunneling rates J, the tendency is for all the atoms to be completely delocalized in all lattice sites.

An optical lattice is generated with standing waves of lasers in the 3 spatial directions turned on atop a Bose-Einstein condensate (BEC). The intensity of the lasers allows to control the quotient $\frac{U}{J}$, and this mechanism permitted experimental demonstration of the SF-MI transition[2]. A property of the MI state that distinguishes it from a fully incoherent state is that it is possible to recover the SF state after elimination of the optical lattice. In addition, it possesses a finite gap with respect to the first excited state. In the case where the filling factor $n = 1$, it is clear that a hop of an atom to its neighboring site requires an energy U. This gap can be explored by introducing a bias μ_i between neighboring sites. When $\mu_i - \mu_{i+1} = U$, the SF phase cannot be recovered, and this situation is associated to the overlap generated with the first excited state in the MI phase.

This is an example of the many simulations of condensed matter systems that have been carried out lately in lattices of cold atoms.

5.2.2 Trapped ions

The natural model to discuss in the case of trapped ions is the simulation of spin chains. This has indeed been explored, for instance, with the intention to explore the transition between paramagnetic and antiferromagnetic phases. A more exotic investigation was the simulation of the Dirac equation in a single trapped ion[3].

The Dirac equation in 3+1 dimensions has the form

$$-i\hbar\frac{d}{dt}\psi = \left(c\boldsymbol{\alpha}\boldsymbol{p} + \beta mc^2\right)\psi = H_D\psi,$$

with $\alpha_i = \begin{pmatrix} 0 & \sigma_i \\ \sigma_i & 0 \end{pmatrix}$ and $\beta = \begin{pmatrix} 1 & 0 \\ 0 & -1 \end{pmatrix}$. The spinor ψ has 4 components, which correspond to the positive and negative relativistic energy values

$$E = \pm\sqrt{p^2c^2 + m^2c^4}$$

and to the spin $\frac{1}{2}$ degree of freedom.

The position of the particle can be derived on the Heisenberg picture

$$\frac{d}{dt}\boldsymbol{x} = \frac{i}{\hbar}\left[H_D, \boldsymbol{x}\right] = c\boldsymbol{\alpha}$$

and

$$\frac{d}{dt}\boldsymbol{\alpha} = \frac{i}{\hbar}\left[H_D, \boldsymbol{\alpha}\right] = 2i\left(c\boldsymbol{p} - \boldsymbol{\alpha}H_D\right)$$

which provides the solution

$$\boldsymbol{x}\left(t\right) = \boldsymbol{x}\left(0\right) + c^2\boldsymbol{p}H_D^{-1}t + \frac{i\hbar c}{2}H_D^{-1}\left(\boldsymbol{\alpha}\left(0\right) - c\boldsymbol{p}H_D^{-1}\right)\left(e^{-2iH_Dt/\hbar} - 1\right).$$

[2] Greiner, M., Mandel, O., Esslinger, T., Hänsch, T. W., & Bloch, I., Nature, 415(6867), (2002).

[3] Lamata, L., León, J., Schätz, T., & Solano, E., Physical Review Letters, 98(25), 253005 (2007).
Gerritsma, R., Kirchmair, G., Zähringer, F., Solano, E., Blatt, R., & Roos, C. F. , Nature, 463(7277), (2010).

Apart from the usual term that evolves linearly with time, we note the existence of an additional, oscillatory term.

The form of the Dirac equation for the 1+1 dimensional case is

$$-i\hbar\frac{d}{dt}\psi = \left(cp\sigma_x + mc^2\sigma_z\right)\psi,$$

which is a Hamiltonian that can be implemented in a trapped ion setting.

The phenomenon of Zitterbewegung, the oscillating behavior of free particles consequence of interference between the positive and negative energy wavefunctions, has not been observed: in the case of electrons, it has an amplitude $R_{ZB} = 10^{-3}$Åand a frequency $\omega_{ZB} = 10^{21}Hz$, which makes it inaccessible. In an ion trap setting, one has to understand the positive and negative energy part of the spinor as the two polarons associated to a spin-boson model. A measurement of the dipole provides access to the position $x(t)$, which reproduces the expected behavior from simulations.

6. Alternative formulations of quantum computation

The realization that systematic errors arising from environmental effects were the main limiting factors for the scalability of quantum computers fueled interest in the formulation of alternative proposals of quantum computation that would be naturally protected from decoherence.

6.1 Adiabatic quantum computation

The understanding of decoherence as a dynamical process favors the idea that encoding the solutions of algorithms in the ground state of a system may constitute a more robust method than subsequent operation with quantum gates. This is the basis of adiabatic quantum computation.

The basic principle one has to follow in order to encode a solution to an algorithm in the ground state of a Hamiltonian is to introduce energetic penalties to states that are known not to constitute a solution. The oracle operator of the Grover search algorithm is a clear example thereof

$$O = (I - 2\left|x\right\rangle\left\langle x\right|).$$

If we understand O as a unitary transformation, it introduces a phase -1 for the solution states $\left|x\right\rangle$. But if we take it as a Hamiltonian, its ground state is the subspace described precisely by these very solution states. If one is able to build a system with Hamiltonian O, it is possible to extract the solution from the state of lowest energy.

The question is how to reach the ground state. A complicated Hamiltonian in isolation need not populate that state easily[1]. Instead of preparing a complicated ground state, a possibility is to start with a much simpler initial Hamiltonian whose ground state is easy to reach and to prepare with high fidelity. One may then slowly drive the initial Hamiltonian through to reach the goal Hamiltonian. The speed of this transformation needs to be slow enough that excited states do not populate in the process. This idea is systematized in terms of the adiabatic theorem

[1] See, for instance, ground state laser cooling of trapped ions.

6.1.1 Adiabatic theorem

Let us consider the evolution of a system under the effect of a time-dependent Hamiltonian

$$\frac{d}{dt}\left|\Psi\left(t\right)\right\rangle = \frac{-i}{\hbar}H\left(t\right)\left|\Psi\left(t\right)\right\rangle.$$

We may define the instantaneous basis

$$H\left(t\right)\left|\phi_n\left(t\right)\right\rangle = \epsilon_n\left(t\right)\left|\phi_n\left(t\right)\right\rangle,$$

with which we may express the formal solution of the Schrödinger equation

$$\left|\Psi\left(t\right)\right\rangle = \sum_n c_n\left(t\right)e^{-i\theta_n}\left|\phi_n\left(t\right)\right\rangle,$$

with $\theta_n = \frac{1}{\hbar}\int_0^t \epsilon_n\left(s\right)ds$. It is possible to derive the following equation for the rate of change of the amplitudes

$$\dot{c}_n = -c_n\left\langle\phi_n\right|\frac{d}{dt}\left|\phi_n\right\rangle - \sum_{m\neq n} c_m\frac{\left\langle\phi_n\right|\dot{H}\left|\phi_m\right\rangle}{E_m - E_n}e^{-i(\theta_m-\theta_n)}. \tag{6.1}$$

The first term is the adiabatic term, which corresponds to an evolution where the probability distribution over the instantaneous basis does not change. The second term is the one that needs to be negligible

$$\sum_{m\neq n} c_m\frac{\left\langle\phi_n\right|\dot{H}\left|\phi_m\right\rangle}{E_m - E_n}e^{-i(\theta_m-\theta_n)} \ll 1.$$

For an initial distribution $c_n = \delta_{n0}$, this translates into the requirement that the rate of change of the form of the Hamiltonian $\dot{H}$ needs to be much smaller than the energy gap $E_1 - E_0$ between the ground and the first excited states. This is how the spectral gap becomes a measure of complexity of an adiabatic quantum algorithm.

Exercise 17

Schein: Derive equation 6.1.

6.1.2 Equivalence with the circuit model of quantum computation

It is possible to show that there is no fundamental computational advantage in using the circuit model of quantum computation or the adiabatic one, in the sense that one can map one into the other with a polynomial overhead[2]. The transformation of an adiabatic algorithm into a circuit is possible through quantum simulation of the adiabatic process in a quantum computer. The less trivial aspect is how to represent a circuit operation in an adiabatic algorithm.

[2] Charles Epstein's notes.

This is possible by attempting to represent the entire history of the quantum computation in a superposition

$$|\eta\rangle \equiv \frac{1}{\sqrt{L+1}} \sum_{j=0}^{L} |\alpha(j)\rangle \left|1^j 0^{L-j}\right\rangle^c,$$

where L is the number of steps of the computation, $|\alpha(j)\rangle$ is the state of the system after the gate j has been applied and $\left|1^j 0^{L-j}\right\rangle^c$ is the "clock" state, that represents the step that is encoded in $|\alpha(j)\rangle$. The algorithm requires n qubits, and therefore $|\alpha(j)\rangle$ is registered equally in n qubits, whereas the clock state requires $L+1$ qubits. Note that, by projecting the clock state in one of its possible values, one recovers the state $|\alpha(j)\rangle$, but otherwise this is just a highly entangled state.

Now we need to find a Hamiltonian whose ground state is $|\eta\rangle$. We will start with a Hamiltonian

$$H_I = H_{clockinit} + H_{clock} + H_{init}$$

with

$$H_{init} = \sum_{i=0}^{n} |1\rangle\langle 1|_i \otimes |0\rangle\langle 0|_1^c$$

which is a term that introduces an energy penalty to all states that do not start with $|0\rangle^{\otimes n}$. The subscript always indicates the qubit upon which the operator acts, superscript c refers to the clock qubits. The clock term of the Hamiltonian ensures only valid clock states can be part of the ground state

$$H_{clock} = \sum_{j=0}^{L} |01\rangle\langle 01|_{j,j+1}^c,$$

since all clock states only contain ones followed by zeros. Finally, the Hamiltonian

$$H_{clockinit} = |1\rangle\langle 1|_1^c$$

ensures that the initial clock state is $|0\rangle^{\otimes L+1}$. This Hamiltonian is adiabatically transformed

$$H(s) = (1-s)H_I + sH_F$$

into the Hamiltonian

$$H_F = \frac{1}{2}\sum_{j=0}^{L} H_j + H_{clock} + H_{init}.$$

The final Hamiltonian contains the terms

$$H_j = I \otimes \left(|100\rangle\langle 100|_{j-1,j,j+1}^c + |110\rangle\langle 110|_{j-1,j,j+1}^c\right) - \left(U_j \otimes |110\rangle\langle 100|_{j-1,j,j+1}^c + h.c\right),$$

where U_j is the gate applied at time-step j.

Exercise 18

Schein: Show that $H_F|\eta\rangle = 0$, and that it is its ground state.

It was shown[3] that this formulation requires an overhead of $O\left(L^5\right)$ and is therefore polynomially equivalent to the circuit model of quantum computation.

6.2 Quantum annealing

The concept of adiabatic quantum computation tries to circumvent the pernicious effect of environmental decoherence by remaining in an "indestructible" state: the ground state. It nevertheless still has to pay the toll of inefficiency in the form of a very long driving time that is dictated by the spectral gap between ground and first excited state. A natural consideration would be to drop the necessity to approach the ground state by adiabatic means.

Clearly, a more natural representation of the dynamics of a system in contact with the environment is provided by thermodynamics. A possibility is to try to approach the ground state by means of a cooling process. In order to increase the chance to reach the ground state, a highly disordered state needs to be the starting point. Instead of using some external adiabatic driving, it is the temperature that is "driven" in order to reach the algorithm result encoded in the ground state. This procedure has been the inspiration to the concept of simulated annealing, which is a stochastic algorithm used in computer science.

The quantum counterpart, quantum annealing, exploits the fluctuations generated by non-commuting terms in the Hamiltonian in order to generate the highly disordered initial state. This is the implementation that seeks to realize the D-Wave, a machine that has gathered much attention since major companies began to invest effort in studying its capabilities. Its central "processing unit" is a network of superconducting circuits.

6.2.1 Classical vs quantum annealing

It is best to regard annealing as an optimization procedure that attempts to search for a fairly good solution to a problem, without a guarantee to reach the best one. In classical annealing, this translates to reaching a favorable state of the system by means of free energy minimization

$$F\left[p\left(x\right)\right] = E\left[p\left(x\right)\right] - TS\left[p\left(x\right)\right],$$

where we picture the thermodynamic potentials (F, free energy; E, inner energy; S, entropy) as functionals of the probability distribution over the system states x. In a high temperature situation, the free energy F is minimized for maximum entropy, i.e. a maximally mixed distribution $p\left(x\right)$. As temperature decreases, the energy landscape E modifies the single minimum of the entropic term into a generally complex situation. Nevertheless, the highly spread initial form of $p\left(x\right)$ allows the system to explore a big range of possible minima and settle in a fairly good solution to the optimization problem.

In the quantum case, fluctuations are not only of thermal nature. Additional fluctuations may be generated by the introduction of a non-commuting Hamiltonian part, so that

$$F_Q\left[p\left(x\right)\right] = Tr\left[H_F\rho\right] + K\left(t\right)Tr\left[H_I\rho\right] - TS\left[\rho\right],$$

[3] D. Aharonov, W. van Dam, J. Kempe, et al., SIAM Review, 50(4):755–787, (2008), arXiv:quant-ph/0405098v2.

where H_F is the Hamiltonian where the solution is encoded and H_I is a controllable Hamiltonian whose strength we can drive by means of $K(t)$. The combination of quantum and thermal fluctuations is believed to accelerate the search for an optimum, since quantum fluctuations allow to tunnel narrow barriers even if they are very high, whereas thermal fluctuations do not allow that. Also, non-local transformations of the state are possible in quantum systems but are more unlikely in the classical case. Nevertheless, no general result exists in this direction and this is a matter of current research.

As is a matter of current research the ability by D-Wave processors to perform quantum annealing. An example Hamiltonian that may be implemented in a D-Wave is an Ising network with a transverse field

$$H = \sum_{i=1}^{N} h_i Z_i + \sum_{i<j=2}^{N} J_{ij} Z_i Z_j + \sum_{i=1}^{N} g_i(t) X_i,$$

where quantum fluctuations are introduced by means of the controls $g_i(t)$ and one may encode a specific energy landscape in the coefficients h_i and J_{ij}. Nevertheless, the claims of quantum speedup on these machines have been heavily contested.

6.3 Measurement based quantum computation

The first protocol that we learnt about in this lecture series, quantum teleportation, may be extended to become a model for universal quantum computation. The central concept involves a highly entangled state upon which measurements are adaptively performed. The final result of the computation is determined by the measurement outcomes. Two main versions exist: teleportation quantum computation (TQC) and one way quantum computation (1WQC). It may appear surprising that collapsing the wave function, thereby obtaining classical information, would be enough to expoit the promise of efficiency of quantum computation. Let us explore the possibilities offered by this perspective.[4]

6.3.1 Teleportation quantum computation

The teleportation protocol consists in a Bell state measurement in two qubits, an input $|\psi\rangle_1$ and one half of a Bell pair (qubit 2 in $|\beta_{00}\rangle_{23}$), in order to transfer the original input state to the other half of the Bell pair (qubit 3 in $|\beta_{00}\rangle_{23}$) up to single qubit gates. For any single-qubit unitary U, let us define the generalized Bell basis elements $|\beta_{ab}(U)\rangle \equiv U^\dagger \otimes I |\beta_{ab}\rangle$. Measurement on that basis with outcome ab will teleport the state $Z^a X^b U |\psi\rangle$ instead. This central idea of carefully choosing the measurement basis to obtain an applied gate on another qubit can be easily extended to higher dimensions, so that multi-qubit gates are also possible.

This can be easily generalized to a sequence of gates. What to do with the unwanted Pauli operators $X^a Z^b$ that depend on the measurement outcome? A possibility to get rid of them is by *adaptive measurement*, that is, adapting the form of subsequent measurements to the

[4] A good overview on the topic is offered by Jozsa, R. arxiv:quant-ph/0508124, (2005).

Exercise 19

Schein: Given the $d-$dimensional maximally entangled state of a two particle system

$$|\phi\rangle = \frac{1}{\sqrt{d}} \sum_{i=1}^{d} |i\rangle |i\rangle ,$$

and a unitary U, define a measurement protocol to teleport the state $U|\phi\rangle$.

outcomes. Let us consider the single-qubit example to clarify this point. Rotations around x and z axes of the Bloch sphere are affected as follows by Pauli operators

$$\begin{aligned} R_x(\theta) X &= X R_x(\theta) , \\ R_x(\theta) Z &= Z R_x(-\theta) , \\ R_z(\theta) X &= X R_z(-\theta) , \\ R_z(\theta) Z &= Z R_z(\theta) . \end{aligned}$$

To perform the measurements correponding to the gate sequence $R_z(\alpha) R_x(\beta)$, one begins by the application of the teleportation protocol for the first gate, which will yield the state $Z^a X^b R_x(\beta)|\psi\rangle$. The second step is to apply the teleportation protocol corresponding to the adaptive gate $R_z\left((-1)^b \alpha\right)$ so that the final state is $Z^{a+c} X^{b+d} R_z(\alpha) R_x(\beta)|\psi\rangle$.

A similar situation occurs for the CZ (controlled phase) gate, with the addition that the gate is not affected by the commutation

$$\begin{aligned} CZ(Z \otimes I) &= (Z \otimes I) CZ, \\ CZ(X \otimes I) &= (X \otimes Z) CZ. \end{aligned}$$

The fact that CZ needs not be adapted to any previous measurement result introduces a new flexibility in this model: the possibility to apply that gate on the required qubits at any point in time.

6.3.2 Clifford operations

Operations that are not adapted to some previous measurment outcome are useful in the sense that they allow us to parallelize the operation of the computation (there is no need to wait for any measurement result to perform that operation). Let us define the Pauli group $\mathcal{P}_n$ as the set of $n$fold tensor products of Pauli matrices, as if they each operated on one of n separate qubits. A unitary C is a Clifford operation if $C\mathcal{P}_n C^\dagger = \mathcal{P}_n$, which formally expresses that, for an element P of $\mathcal{P}_n$, $CP = P'C$, with P' another element of $\mathcal{P}_n$. We have already noted that CZ is a Clifford operation, and so is the Hadamard gate, the $\pi/4$-phase gate T^2 and Z. These are sufficient to express any unitary operation to arbitrary accuracy. As opposed to the circuit model of quantum computation, a set of Cllifford operations does not need to be applied one step after the other, but all in parallel, plus a classical computation to deduce the residual Pauli matrices to the left of the desired quantum operation. This separation into an "easy" quantum operation and a classical operation facilitates the characterization of the bare minimum quantum ressources required to preform a quantum operation.

6.3.3 One way quantum computation

One way quantum computation (1WQC) requires a cluster state to operate on. A cluster state is defined on top of a graph whose nodes are qubits in the $|+\rangle$ states and the edges are the application of an entangling CZ gate. The computation proceeds with the appication of measurements either in the Z or the X basis. Other measurment bases would do a similar job, but let us stick to the conventional choice.

Let us regard the example of teleportation in 1WQC. Given a state $|\psi\rangle$, adjoin $|+\rangle$, entangle with CZ and X-measure the first qubit, giving and outcome s and leaving the second qubit in state $X^sH|\psi\rangle$. Performing the same steps with the second qubit and an additional third qubit would leave the third qubit in state $X^rHX^sH|\psi\rangle = X^rZ^s|\psi\rangle$, where r is the outcome of measurement of qubit 2. We have an outcome that is very similar to the teleportation protocol, where only CZ and local measurements took place. This is not a big surprise if one realizes that the sequence of gates just described is a reordering of the quantum teleportation protocol for local measurement (Fig.2.2). In general, one may reorder the CZ gates involved in a calculation to the beginning (creation of the cluster state) and perform local measurements according to the required effects. An interesting aspect is the role of measurements in the Z basis is to decouple that node from the rest of the graph.

6.4 Topological quantum computation

The use of physically protected degrees of freedom for the implementation of quantum information processing has its best example in the concept of topological quantum computation. Here, exchange statistics of particles are exploited in order to represent unitary transformations.

6.4.1 Physical support

In three dimensions, there exists only two types of exchange statistics: bosonic and fermionic. Two indistinguishable particles that are exchanged look exactly the same as before, but it is known that their wavefunction acquires a phase -1 if the particles are fermions.

The Aharonov-Bohm effect is a related phenomenon. A particle of charge e that is confined in a plane gains an overall phase $e^{i\phi e}$ when it encircles a section with magnetic flux ϕ. This is a non-trivial exchange phase that does not correspond neither to bosons (trivial phase) or fermions (phase -1). For this reason, one may consider the set of flux and charged particle as a new particle with a special exchange statistics: an anyon. This phase is stable under the deformation of the trajectory, so it is said to be topologically protected, and this is the reason why it is thought to be an indicated degree of freedom. In three dimensions, trajectories may be deformed topologically into a point, so none of these effects take place.

The classical quantum Hall effect involves the generation of a potential between two ends of a metallic slab that is in a magnetic field. The quantum case involves fractional values of charge that can be used as topological degrees of freedom.

6.4.2 Flux-charge systems

Let us consider a two-dimensional superconducting material that has a region where magnetic flux Φ is non-zero. This region is impenetrable to charges in the superconductor, and magnetic flux across a superconductor must be zero. By means of the Aharonov-Bohm effect, an electric charge q transported around the flux acquires a topological phase

$$U(2\pi) = e^{-i2\pi\mathbf{J}} = e^{iq\Phi}$$

where $\mathbf{J}$ is the angular momentum. The equality imposes the following possible eigenvalues of angular momentum

$$J = m - \frac{q\Phi}{2\pi}$$

and we may define the angular variable as the intrinsic spin of the flux-charge composite system $\theta = q\Phi \pmod{2\pi}$ so that the topological phase is $e^{i\theta}$. This allows us to consider this system as an anyon: a particle that does not follow bosonic nor fermionic statistics.

Let us introduce the concept of braiding. Given a number n of these anyons, how can we best represent the effects of arbitrary exchanging of particles? We may represent the evolution of the system as a world-line, where the position of the particle is followed and forms a line in a 2+1 space. Exchanges of particles appear then like braiding of the several threads and can be represented by permutation operators σ_j, that corresponds to the counterclockwise exchange of particles j and $j+1$. These operators form the Braid group and the algebra they follow is defined by

$$\sigma_j\sigma_k = \sigma_j\sigma_k,$$

for $|j-k| \geq 2$, which states that exchanging two disjoint pairs commutes, and

$$\sigma_j\sigma_{j+1}\sigma_j = \sigma_{j+1}\sigma_j\sigma_{j+1},$$

known as the Yang-Baxter relation.

A one dimensional representation of this group corresponds to $\sigma_j = e^{i\theta_j}$. The Yang-Baxter relation implies $\theta_j = \theta_k = \theta$, which makes sense for indistinguishable particles.

Exercise 20

Schein: Show graphically that the Yang-Baxter relation holds and justify that all exchange phases of the one-dimensional representation of the braid group are equal.

The more interesting non-abelian representations of this group will provide us with the possibility to perform quantum computation.

6.4.3 Non-Abelian topological transformations

Let a non-abelian finite group G the group of values that flux can take and charges unitary irreducible representations of this group. Let R a particular irreducible representation of G of dimension $|R|$ with an arbitrary orthonormal basis

$$|R,i\rangle, \quad i = 1,2,\ldots,|R|.$$

When going around a flux $a \in G$, the charge transforms by means of a unitary matrix $D^R(a)$ in the form

$$|R,j\rangle \to \sum_{i=1}^{|R|} |R,i\rangle\, D^R_{ij}(a)\,.$$

Let us assume we have two fluxes, each corresponding to an element in G. The transformation rule for flux exchange follows

$$|a,b\rangle \to \left|b, b^{-1}ab\right\rangle,$$

which one can be convinced about with the help of a test charge winding around each of the two fluxes and the deformation the winding path suffers due to the exchange of fluxes.

Knowing how the braiding operator acts on fluxes allows one to develop the whole algebra of a specific topological model. Specifically, it is possible to associate charge to certain flux states, which in turn is associated to fusion or annihilation rules.

The general scheme of a topological quantum computation involves the generation of flux pairs, their braiding as a means to effectively implement quantum gates and measurement of the outcome by fusioning the outcoming fluxes.

6.4.4 Quantum Hall effect

The classical Hall effect consists in the build up of a potential across the direction of a current in the presence of a strong magnetic field. Its quantized form involves the free Hamiltonian

$$H = \frac{\boldsymbol{\pi}^2}{2m*} = \frac{(\mathbf{p}+e\mathbf{A})^2}{2m^*},$$

where m^* is the effective mass of the electron in the conductor. For a two-dimensional geometry and a vector field $\mathbf{A} = -Bx\hat{\mathbf{y}}$ (Landau gauge)

$$H = \frac{p_x^2}{2m^*} + \frac{(p_y - eBx)^2}{2m^*}.$$

Whereas the y part of the wavefunction (along the conduction axis) may be described with plane waves, the x part takes the form of a harmonic well centered at a point proportional to the y momentum. These harmonic wells produce quantized levels, which are known as the Landau levels. Each eigenstate in the conduction direction y has an associated harmonic well. Assuming periodic boundary conditions for the p_y eigenstates and a length L of the conductor, the distance between two harmonic wells is

$$\frac{2\pi\hbar}{LeB}$$

and the associated flux

$$\frac{2\pi\hbar}{LeB}LB = \frac{h}{e},$$

ie, a flux quantum. Each harmonic well is separated by a flux quantum, so that the number of flux quanta is associated to the number of orthogonal states in the sample. The filling factor ν is the quotient between the carrier density and the number of flux quanta, or how many

electrons there are per state. The phenomenon of edge states being the ones carrying current is present in this system, and corresponds to integer filling factors.

For fractional filling factors, it is useful to use the symmetric gauge instead $\mathbf{A} = -Bx\hat{\mathbf{y}} + iBy\hat{\mathbf{x}}$. A ground state ansatz for a filling function is the Laughlin wavefunction, which makes sure that electrons are as far apart as possible. This can be interpreted as associating electrons to flux quanta in such a way that composite particles with fractional charge arise.

7. Environmental effects

The performance of quantum computers is strongly perturbed by the effects of the environment. Let us formalize the study of these effects with the help of the theory of open quantum systems.

7.1 Dynamical map

The reduced description of a system in contact with an environment is a useful tool for the study of detrimental effects on coherent operations. Its central object is the reduced density matrix of the system, and its evolution is dictated by the dynamical map, an object analogous to the evolution operator for wavefunctions. For separable initial conditions between the system and the environment, it is the map $\mathcal{E}$ between the initial state of the system $\rho(0)$ and the final one $\rho(t)$

$$\rho(t) = \mathcal{E}\rho(0).$$

It inherits properties from the density matrices: it is a trace-preserving map and it is completely positive. Complete positivity is a stronger property than positivity, and it requires that the same map applied to any extension of the system is also positive.

Exercise 21
Schein: show that the transpose map is not completely positive

The generation of the dynamical from a microscopic description of the environment is not trivial, although it can be done for simple cases. Let us look at the example of the dephasing channel, where the energy splitting between the two levels of a qubit is perturbed by coupling to an environment of harmonic oscillators. The Hamiltonian for this model has the form

$$H = H_S + H_{SB} + H_B = \sigma_z \left(\omega + \sum_k g_k \left(a_k + a_k^\dagger \right) \right) + \sum_k \nu_k a_k^\dagger a_k$$

and compute the dynamical map elements

$$\mathcal{E}_{ij} = Tr \left\{ \sigma_i U \sigma_j \otimes \rho_B U^\dagger \right\},$$

where $\rho_B = e^{-\beta H_B}/Z$ and $\sigma_i \in \{|e\rangle\langle e|, |g\rangle\langle e|, |e\rangle\langle g|, |g\rangle\langle g|\}$ a basis in the system's operator space. The computation requires the evolution operator

$$U = e^{-it(\omega\sigma_z + \sigma_z X + H_B)},$$

with $X = \sum_k g_k \left(a_k + a_k^\dagger\right)$. It is clear from the form that U can only have diagonal elements in the $\{|e\rangle, |g\rangle\}$ basis, which propagates to a form of $\mathcal{E}_{ij}$ in the σ_i basis with only 4 non-vanishing entries.

Let's define the displacement operator as

$$D(\alpha_k) = \exp\left(\sum_k \left(\alpha_k a_k - \alpha_k^\dagger a_k^\dagger\right)\right),$$

and use the shorthand notation for the polaron transformation

$$D^{P\pm} = \exp\left(\pm\sigma_z \sum_k \frac{g_k}{\omega_k}\left(a_k - a_k^\dagger\right)\right),$$

and

$$D^{\pm} = \exp\left(\pm \sum_k \frac{g_k}{\omega_k}\left(a_k - a_k^\dagger\right)\right),$$

such that

$$U = e^{-it\omega\sigma_z} D^{P+} e^{-itH_B} D^{P-},$$

up to a global phase that is not relevant for the dynamical map. The four non-vanishing elements of the dynamical map are

$$\begin{aligned}
\mathcal{E}_{11} &= 1, \\
\mathcal{E}_{23} &= e^{-2it\omega} Tr\left\{D^+ e^{-itH_B} D^- \rho_B D^- e^{itH_B} D^+\right\}, \\
\mathcal{E}_{32} &= e^{2it\omega} Tr\left\{D^- e^{-itH_B} D^+ \rho_B D^+ e^{itH_B} D^-\right\}, \\
\mathcal{E}_{44} &= 1.
\end{aligned}$$

As an example, let us compute one of the non-trivial explicitly. For a scalar dependence of the displacement operator

$$D(\alpha_k) = \exp\left(\sum_k \left(\alpha_k a_k - \alpha_k^* a_k^\dagger\right)\right),$$

it has the properties

$$D(\alpha_k) D(\beta_k) = D(\alpha_k + \beta_k) \exp\left\{-i \sum_k \Im\left[\alpha_k \beta_k^*\right]\right\},$$

and

$$\langle D(\alpha_k)\rangle = \exp\left\{-\frac{1}{2}\sum_k |\alpha_k|^2 \coth\left[\frac{\beta\omega_k}{2}\right]\right\}.$$

Exercise 22
Schein: Derive the properties of the displacement operator

The element looks

$$\begin{aligned}\mathcal{E}_{23} &= e^{-2it\omega} Tr\left\{D\left(-\frac{g_k}{\omega_k}\right) D\left(2\frac{g_k}{\omega_k}e^{-i\omega_k t}\right) D\left(-\frac{g_k}{\omega_k}\right)\rho_B\right\}, \\ &= e^{-2it\omega}\exp\left\{-4\sum_k \frac{g_k^2}{\omega_k^2}\left(1-\cos\omega_k t\right)\coth\left[\frac{\beta\omega_k}{2}\right]\right\}\end{aligned}$$

so that

$$\mathcal{E}_{32} = e^{2it\omega}\exp\left\{-4\sum_k \frac{g_k^2}{\omega_k^2}\left(1-\cos\omega_k t\right)\coth\left[\frac{\beta\omega_k}{2}\right]\right\}.$$

Let us define the correlation function $C_2(t) = \sum_k \frac{g_k^2}{\omega_k^2}\cos\omega_k t\coth\left[\frac{\beta\omega_k}{2}\right]$ so that

$$\mathcal{E}_{32} = e^{2it\omega}\exp\left\{-4\left[C_2(0) - C_2(t)\right]\right\}.$$

In general, the norm of $\mathcal{E}_{32}$ approaches a steady state value close to zero determined by $C_2(0)$. Correlation functions that take negative values will see a norm that does not decay monotonically to the steady state but rather take a low value that then slowly increases until the steady state.

7.2 Nakajima-Zwanzig equation

It is not always possible to derive an analytical form of the dynamical map. In general, it follows a formal equation that can be derived with help of projection operators on the relevant Hilbert subspace $\mathcal{P}$ and its complement $\mathcal{Q} = 1 + \mathcal{P}$. Let us start with a Schrödinger equation for the system and the bath

$$\frac{d}{dt}|\Psi\rangle = -i\hbar H|\Psi\rangle$$

and its generalization for the density matrix $\sigma = |\Psi\rangle\langle\Psi|$

$$\frac{d}{dt}\sigma = \left(\frac{d}{dt}|\Psi\rangle\right)\langle\Psi| + |\Psi\rangle\left(\frac{d}{dt}\langle\Psi|\right) = -\frac{i}{\hbar}H|\Psi\rangle\langle\Psi| + \frac{i}{\hbar}|\Psi\rangle\langle\Psi|H = -\frac{i}{\hbar}[H,\sigma],$$

which is known as the Liouville equation. In Liouville space it takes the form

$$\frac{d}{dt}\sigma = \mathcal{L}\sigma,$$

one has

$$\frac{d}{dt}\mathcal{P}\sigma = \mathcal{P}\mathcal{L}\left(\mathcal{P}+\mathcal{Q}\right)\sigma,$$
$$\frac{d}{dt}\mathcal{Q}\sigma = \mathcal{Q}\mathcal{L}\left(\mathcal{P}+\mathcal{Q}\right)\sigma.$$

Formal integration of the second equation

$$\mathcal{Q}\sigma\left(t\right) = \exp\left(\mathcal{Q}\mathcal{L}t\right)\mathcal{Q}\sigma\left(0\right) + \int_0^t \exp\left[\mathcal{Q}\mathcal{L}\left(t-t'\right)\right]\mathcal{Q}\mathcal{L}\mathcal{P}\sigma\left(t'\right)dt'$$

can be used to derive an integro-differential equation for $\mathcal{P}\sigma\left(t\right)$

$$\frac{d}{dt}\mathcal{P}\sigma = \mathcal{P}\mathcal{L}\mathcal{P}\sigma + \mathcal{P}\mathcal{L}\mathcal{Q}\exp\left(\mathcal{Q}\mathcal{L}t\right)\mathcal{Q}\sigma\left(0\right) + \int_0^t \mathcal{P}\mathcal{L}\mathcal{Q}\exp\left[\mathcal{Q}\mathcal{L}\left(t-t'\right)\right]\mathcal{Q}\mathcal{L}\mathcal{P}\sigma\left(t'\right)dt',$$

In order to avoid the convolution term, we may connect the state of the system at two different times with help of the unitary inverse evolution $\exp\left[-\mathcal{L}\left(t-t'\right)\right]$

$$\mathcal{P}\sigma\left(t'\right) = \mathcal{P}\exp\left[-\mathcal{L}\left(t-t'\right)\right]\left(\mathcal{P}+\mathcal{Q}\right)\sigma\left(t\right).$$

Now we may define

$$\Sigma\left(t\right) = \int_0^t \exp\left[\mathcal{Q}\mathcal{L}\left(t-t'\right)\right]\mathcal{Q}\mathcal{L}\mathcal{P}\exp\left[-\mathcal{L}\left(t-t'\right)\right],$$

and therefore

$$\left[1+\Sigma\left(t\right)\right]\mathcal{Q}\sigma\left(t\right) = \exp\left(\mathcal{Q}\mathcal{L}t\right)\mathcal{Q}\sigma\left(0\right) + \Sigma\left(t\right)\mathcal{P}\sigma\left(t\right),$$

so that introduction in the differential equation for $\mathcal{P}\sigma$ yields

$$\frac{d}{dt}\mathcal{P}\sigma = \mathcal{P}\mathcal{L}\mathcal{P}\sigma + \left[1+\Sigma\left(t\right)\right]^{-1}\left[\exp\left(\mathcal{Q}\mathcal{L}t\right)\mathcal{Q}\sigma\left(0\right) + \Sigma\left(t\right)\mathcal{P}\sigma\left(t\right)\right],$$

One usually takes the projector $\mathcal{P}\sigma(t) = Tr_B\left[\sigma(t)\right]\otimes\rho_{B,eq}$, although the derivations so far were fully general.

7.3 Master equation and Born-Markov approximation

Let us derive in a few steps a useful form of the master equation. Although it can be seen as a consequence of the Nakajima-Zwanzig equation, let us illustrate here another pathway for its derivation that is commonly used. Given the splitting of the Hamiltonian

$$H = H_S + H_B + V,$$

in system, bath (environment) and interaction terms, we may define the interaction picture with respect to the free part of the Hamiltonian $H_S + H_B$, and derive its associated Liouville equation

$$\frac{d}{dt}\sigma_I = -\frac{i}{\hbar}\left[V_I(t), \sigma_I\right],$$

formal integration provides

$$\sigma_I(t) = \sigma_I(0) - \frac{i}{\hbar}\int_0^t dt' \left[V_I(t'), \sigma_I(t')\right].$$

We are interested in the system dynamics, so we define the partial trace with respect to the bath degrees of freedom.

$$\rho = Tr_B[\sigma],$$

Interaction picture does not modify the elements within the trace, so that a second iteration of the formal solution provides

$$\rho_I(t) = \rho_I(0) - \frac{i}{\hbar}\int_0^t dt' Tr_B\left[V_I(t'), \sigma_I(0)\right] - \left(\frac{i}{\hbar}\right)^2 \int_0^t \int_0^{t'} dt' dt'' Tr_B\left[V_I(t'), \left[V_I(t''), \sigma_I(t'')\right]\right].$$

So far, no approximation was used, but this is as intractable as the Nakajima-Zwanzig equation. It is necessary to apply the Born Markov approximations to obtain a manageable equation.

Assuming a small interaction strength V, it represents a small correction to the free evolution $\sigma_f(t) = \rho_f(t) \otimes \xi_f(t)$. For this reason, the bath is not affected by the evolution and remains in its initial state $\xi = \xi(0)$, which is usually assumed to be the Boltzmann state and therefore commutes with H_B. To first order, the correction contains terms of the form $\langle B\xi(0)\rangle$, which vanishes for harmonic baths with displacing interactions. The second correction is

$$\frac{d}{dt}\rho_I(t) = -\left(\frac{i}{\hbar}\right)^2 \int_0^t dt' Tr_B\left[V_I(t), \left[V_I(t'), \rho_I(t') \otimes \xi(0)\right]\right],$$

and constitutes the Born approximation.

The second approximation (Markov) has to do with the correlation time of the bath. The most general form of the interaction Hamiltonian is $V = \hbar\sum_k S_k B_k$, so that the partial trace is proportional to the correlation functions

$$C_{kn}(t, t') = Tr\left[B_{k,I}(t) B_{n,I}(t')\xi\right],$$

which only depend on $t - t'$ because of the cyclic property of the trace and because ξ commutes with H_B. Therefore

$$\frac{d}{dt}\rho_I(t) = \int_0^\infty dt' \sum_{k,n} \left\{C_{kn}(t - t')\left[S_{k,I}(t), S_{n,I}(t')\rho_I(t)\right] + C_{nk}(t' - t)\left[\rho_I(t) S_{n,I}(t'), S_{k,I}(t)\right]\right\},$$

where the Markov approximation assumes $C_{kn}(t) \simeq 0$ for $t < 0$ and $\rho_I(t') \simeq \rho_I(t)$ due to the fast decay of $C_{kn}(t)$. Therefore

$$\frac{d}{dt}\rho = -\frac{i}{\hbar}\left[H_S, \rho\right] + \sum_k \left\{\left[S_k, D_k\rho\right] + \left[\rho E_k, S_k\right]\right\},$$

where

$$D_k \equiv \int_0^\infty d\tau \sum_n C_{kn}(\tau) S_{n,I}(-\tau),$$

$$E_k \equiv \int_0^\infty d\tau \sum_n C_{nk}(-\tau) S_{n,I}(-\tau).$$

The exact form of D_k and E_k depends now exclusively on the microscopic details of the Hamiltonian.

In the spin-boson model the bath takes the form of an infinite collection of harmonic oscillators. Each one is associated to an annihilation operator a_k, where k identifies the mode. The system contains two levels and the interaction takes the form

$$V_{nRWA} = \hbar(S + S^\dagger) \sum_k \gamma_k (a_k + a_k^\dagger),$$

with $\sigma_x = S + S^\dagger$. The interaction picture introduces rotating terms which can be neglected in the appropriate limit (RWA), so that the interaction becomes

$$V_{RWA} = \hbar S \sum_k \gamma_k a_k^\dagger + \hbar S^\dagger \sum_k \gamma_k a_k.$$

This particular interaction involves only two terms so that only four correlation functions appear. Thus, taking ω_k as the frequency of each mode, $\rho(\omega) \equiv \sum_k \gamma_k^2 \delta(\omega - \omega_k)$ the spectral density and $n_B(\omega_k) \equiv Tr_B[a_k^\dagger a_k \xi]$ equilibrium occupation of each mode,

$$C_{12}(t) = Tr_B \left[\sum_{k,k'} \gamma_k \gamma_{k'} a_k e^{-i\omega_k t} a_{k'}^\dagger \xi \right] = \sum_k \gamma_k^2 e^{-i\omega_k t}(1+n_B(\omega_k)) = \int_0^\infty d\omega \rho(\omega) e^{-i\omega t}(1+n_B(\omega)),$$

and, analogously,

$$C_{21}(t) = \int_0^\infty d\omega \rho(\omega) e^{i\omega t} n_B(\omega).$$

The remaining correlations vanish $C_{11}(t) = C_{22}(t) = 0$.

Now it is possible to compute

$$D_1 = \int_0^\infty d\tau C_{12}(\tau) S_{2,I}(-\tau) = \int_0^\infty d\tau C_{12}(\tau) S e^{i\nu\tau} = \hat{C}_{12}(-i\nu) S,$$

where $\hbar\nu$ is the energetic difference between two levels in the system and $\hat{f}$ is the Laplace transform of f. Similarly

$$\begin{aligned} D_2 &= \hat{C}_{21}(i\nu) S^\dagger \\ E_1 &= D_2^\dagger, \\ E_2 &= D_1^\dagger. \end{aligned}$$

Distribution theory allows for the solution of the Laplace transform of the correlation functions, which can be split into an imaginary and a real parts. Imaginary part contributes to the coherent dynamics of the system and turns into a frequency shift of the system (Lamb shift). The real part gives rise to dissipative terms of Lindblad form. In particular

$$\hat{C}_{12}(-i\nu) = \int_0^\infty d\omega \rho(\omega)(1 + n_B(\omega)) \left[\pi\delta(\nu - \omega) + iP\left(\frac{1}{\nu - \omega}\right) \right],$$

so that

$$\Re C_{12}(-i\nu) = \pi\rho(\nu)(1+n_B(\nu)) \equiv \frac{\gamma}{2}(1+\bar{n}_B),$$
$$\Im C_{12}(-i\nu) = P\int_0^\infty d\omega\rho(\omega)\frac{1+n_B(\omega)}{\nu-\omega} \equiv \Delta_1.$$

Analogously

$$\Re C_{21}(i\nu) = \pi\rho(\nu)n_B(\nu) \equiv \frac{\gamma}{2}\bar{n}_B,$$
$$\Im C_{21}(i\nu) = -P\int_0^\infty d\omega\rho(\omega)\frac{n_B(\omega)}{\nu-\omega} \equiv \Delta_2.$$

After redefinition of the system frequency due to the Lamb shifts ($\bar{\nu} \equiv \nu + \Delta_1 + \Delta_2$), the final form of the equation is

$$\begin{aligned}\frac{d}{dt}\rho &= -i\left[\bar{\nu}S^\dagger S,\rho\right] + \frac{\gamma}{2}(1+\bar{n}_B)\left(2S\rho S^\dagger - S^\dagger S\rho - \rho S^\dagger S\right) + \frac{\gamma}{2}\bar{n}_B\left(2S^\dagger\rho S - SS^\dagger\rho - \rho SS^\dagger\right) \\ &= -i\left[\bar{\nu}S^\dagger S,\rho\right] + \frac{\gamma}{2}(1+\bar{n}_B)\mathcal{D}\left[S,\rho\right] + \frac{\gamma}{2}\bar{n}_B\mathcal{D}\left[S^\dagger,\rho\right].\end{aligned} \tag{7.1}$$

In this master equation we can observe a coherent part, describing the dynamics of the system as in the Liouville equation. Additionally, two dissipative terms have appeared. One of them represents "heating" of the system, whereas the other one represents "cooling".

7.4 Decoherence free subspaces

Having the basic tools to model environmental effects, it is now the turn to come up with strategies to fight them. There is a large class of methods and concepts that attempt to tackle this issue, here we will present a few of them. First of all, the concept of decoherence-free subspaces constitutes a passive mechanism to avoid the action of the environment. The underlying idea is that, given a specific form of the system-environment coupling, very often there exist some degrees of freedom of the system that are not affected by it.[1]

Let us consider a system-bath interaction of the form

$$H_{SB} = \sum_{i,k}\left[g^z_{i,k}\sigma^z_i \otimes \left(b_k + b_k^\dagger\right) + g^+_{i,k}\sigma^+_i \otimes b_k + g^-_{i,k}\sigma^-_i \otimes b_k^\dagger\right],$$

which represents a collection of qubits undergoing dephasing and energy exchange with an environment of harmonic oscillators. Assuming all spins couple equally to the baths ($g^\alpha_{i,k} = g^\alpha_k$), one may simplify the appearance of the interaction with

$$H_{SB} = \sum_{\alpha\in\{+,-,z\}} S_\alpha \otimes B_\alpha,$$

[1] Partly based on Lidar, DA, arXiv:1208.5791v2 (2012).

where $S_\alpha = \sum_i \sigma_i^\alpha$ and $B_z = \sum_k g_k^z \left(b_k + b_k^\dagger\right)$, $B_+ = \sum_k g_k^+ b_k$ and $B_- = \sum_k g_k^- b_k^\dagger$. It can be shown that the subspace spanned by the simultaneous eigenstates of all the S_α evolves following unitary dynamics. For this specific example, it corresponds to the vanishing total spin subspace $\left|\vec{S}\right|^2 = 0$, since that ensures that all operators S_α have vanishing eigenvalues. The size d_N of this subspace increases with the number of spins in the form

$$d_N = \frac{N!}{(N/2)!\,(N/2+1)!}$$

for N even. In particular, for 4 qubits, $d_N = 2$ and the decoherence free subspace is spanned by the basis

$$\begin{aligned}
|\bar{0}\rangle &= \frac{1}{2}\left(|0101\rangle - |0110\rangle - |1001\rangle + |1010\rangle\right), \\
|\bar{1}\rangle &= \frac{1}{\sqrt{3}}\left(|0011\rangle + |1100\rangle - \frac{1}{2}|1001\rangle - \frac{1}{2}|0110\rangle - \frac{1}{2}|1010\rangle - \frac{1}{2}|0101\rangle\right).
\end{aligned}$$

Qubits encoded in this two-dimensional space are therefore protected from the environmental effects defined above. It is now necessary to define manners to operate on them. Let us consider E_{ij} the operation that exchanges the values of qubits i and j. It can be easily seen that

$$\begin{aligned}
-E_{12}\,|\bar{0}\rangle &= |\bar{0}\rangle, \\
-E_{12}\,|\bar{1}\rangle &= -|\bar{1}\rangle,
\end{aligned}$$

so that $-E_{12}$ can be seen as a Z operator on this subspace. Similarly, $\frac{1}{\sqrt{3}}(E_{23} - E_{13})$ acts as an X operator. This is enough to generate all single qubit operations to arbitrary accuracy.

In general, given a specific noise model or interaction with the environment, one would hope to find decoherence free subspaces where quantum operations are protected from environmental effects. This is nevertheless not always possible, and a generalization of the idea reduces the restrictions to find protected spaces: noiseless subsystems.

In this case, the Hilbert space is divided in subspaces which have the tensor product form of two subsystems, one of which is free from environmental effect. Given a general system-environment Hamiltonian $H_{SB} = \sum_\alpha S_\alpha \otimes B_\alpha$, the †-closed algebra generated by all system operators $\mathcal{A} = \{S_\alpha\}$ including the identity has the form

$$\mathcal{A} \simeq \bigoplus_J I_{n_J} \otimes \mathcal{M}_{d_J}(\mathbb{C}),$$

so that the Hilbert space of the system can be decomposed in

$$\mathcal{H}_S = \bigoplus_J \mathbb{C}^{n_J} \otimes \mathbb{C}^{d_J},$$

where n_J and d_J mark the dimensionality of the subsystems and $\mathbb{C}^{n_J}$ is not affected by H_{SB}. The decoherence free subspace arises when $d_J = 1$. That this constitutes a generalization can be seen in the fact that this allows to encode a qubit in $N = 3$ physical qubits in the case studied above for decoherence. Decoherence free subspaces would not have allowed it, since there is no $S = 0$ subspace.

7.5 Dynamical decoupling

What we have explored so far is a passive scheme that looks for symmetries in the system-environment Hamiltonian to discover subspaces that are not affected by it. An alternative is to actively generate these symmetries by acting on the system with an external driving.

Let us first consider the example of pure dephasing

$$H_{SB} = \sigma^z B_z$$

and the possibility to drive the system externally

$$H_S = \lambda(t)\,\sigma_x.$$

In the impulsive limit where the system is driven very strongly with intensity λ for a very short period of time $\delta \to 0$ so that $\lambda\delta = \frac{\pi}{2}$, it is possible to represent the evolution due to the pulse as the effect of the system Hamiltonian alone. A sequence of pulses with a time interspacing τ can be represented as

$$X f_\tau X f_\tau \ldots$$

where $f_\tau = e^{-i\tau H_{SB}}$. Due to the rule $XZX = -Z$, the sequence above is equal to unity. Therefore, it is possible to stroboscopically do away with the effect of the environment.

This initial idea has been systematized for general coupling Hamiltonians.

A. Summary of notation and important identities

Pauli matrices

$$X \equiv \sigma_x \equiv \begin{pmatrix} 0 & 1 \\ 1 & 0 \end{pmatrix},$$
$$Y \equiv \sigma_y \equiv \begin{pmatrix} 0 & -i \\ i & 0 \end{pmatrix},$$
$$Z \equiv \sigma_z \equiv \begin{pmatrix} 1 & 0 \\ 0 & -1 \end{pmatrix}.$$

Bell states

$$|\beta_{00}\rangle \equiv \frac{1}{\sqrt{2}} \left(|00\rangle + |11\rangle\right),$$
$$|\beta_{01}\rangle \equiv \frac{1}{\sqrt{2}} \left(|01\rangle + |10\rangle\right),$$
$$|\beta_{10}\rangle \equiv \frac{1}{\sqrt{2}} \left(|00\rangle - |11\rangle\right),$$
$$|\beta_{11}\rangle \equiv \frac{1}{\sqrt{2}} \left(|01\rangle - |10\rangle\right).$$

Hadamard Gate

$$H = \tfrac{1}{\sqrt{2}} \begin{pmatrix} 1 & 1 \\ 1 & -1 \end{pmatrix}$$

$\pi/8$ Gate

$$T = \begin{pmatrix} 1 & 0 \\ 0 & e^{i\pi/4} \end{pmatrix}$$

Bloch sphere: any two-level pure state may be expressed as a point on the surface of a sphere described by the spherical coordinates θ and ϕ

$$|\Psi\rangle = \cos\frac{\theta}{2}|0\rangle + e^{i\phi}\sin\frac{\theta}{2}|1\rangle,$$

where $|0\rangle$ and $|1\rangle$ are the north and south poles of the sphere respectively.

Any **unitary operation** on a two level system can be expressed as

$$R_{\hat{\mathbf{n}}}(\theta) = e^{i\hat{\mathbf{n}}\boldsymbol{\sigma}\frac{\theta}{2}} = \cos\frac{\theta}{2} + i\hat{\mathbf{n}}\boldsymbol{\sigma}\sin\frac{\theta}{2}$$

where $\hat{\mathbf{n}}$ is a unit vector and $\boldsymbol{\sigma} = (\sigma_x, \sigma_y, \sigma_z)$.

Given two unit vectors $\hat{\mathbf{n}}$ and $\hat{\mathbf{m}}$, there always exists a **decomposition**

$$U = e^{i\alpha} R_{\hat{\mathbf{n}}}(\beta) R_{\hat{\mathbf{m}}}(\gamma) R_{\hat{\mathbf{n}}}(\delta).$$

B. Solutions to the exercises

Exercise 1 A general state $|\zeta\rangle$ may be written in terms of the computational basis as $|\zeta\rangle = a_\zeta |0\rangle + b_\zeta |1\rangle$. Therefore

$$\begin{aligned} |\zeta\rangle_A |\xi\rangle_B &= (a_\zeta |0\rangle_A + b_\zeta |1\rangle_A)(a_\xi |0\rangle_B + b_\xi |1\rangle_B) \\ &= a_\zeta a_\xi |0\rangle_A |0\rangle_B + a_\zeta b_\xi |0\rangle_A |1\rangle_B + b_\zeta a_\xi |1\rangle_A |0\rangle_B + b_\zeta b_\xi |1\rangle_A |1\rangle_B . \end{aligned}$$

In order for $|\zeta\rangle_A |\xi\rangle_B = |\Phi\rangle = \frac{1}{\sqrt{2}}(|0\rangle_A |0\rangle_B + |1\rangle_A |1\rangle_B)$ it must happen that

$$\begin{aligned} a_\zeta a_\xi &= \frac{1}{\sqrt{2}}, \qquad a_\zeta b_\xi = 0, \\ b_\zeta b_\xi &= \frac{1}{\sqrt{2}}, \qquad b_\zeta a_\xi = 0. \end{aligned}$$

This system of equations cannot hold simultaneously and, therefore, $|\Phi\rangle$ cannot be expressed in terms of a separable state.

Exercise 2 One just needs to develop the equations (let us drop the party labeling, since the order makes it implicit)

$$\begin{aligned} |\psi\rangle |\Phi\rangle &= \frac{1}{\sqrt{2}}(\alpha |0\rangle + \beta |1\rangle)(|0\rangle |0\rangle + |1\rangle |1\rangle) \\ &= \frac{2}{2\sqrt{2}}(\alpha |0\rangle |0\rangle |0\rangle + \alpha |0\rangle |1\rangle |1\rangle + \beta |1\rangle |0\rangle |0\rangle + \beta |1\rangle |1\rangle |1\rangle) \\ &+ \frac{1}{2\sqrt{2}}(\alpha |1\rangle |1\rangle |0\rangle + \alpha |1\rangle |0\rangle |1\rangle + \beta |0\rangle |1\rangle |0\rangle + \beta |0\rangle |0\rangle |1\rangle) \\ &- \frac{1}{2\sqrt{2}}(\alpha |1\rangle |1\rangle |0\rangle + \alpha |1\rangle |0\rangle |1\rangle + \beta |0\rangle |1\rangle |0\rangle + \beta |0\rangle |0\rangle |1\rangle) \end{aligned}$$

$$
\begin{aligned}
&= \frac{1}{2\sqrt{2}} \left(|00\rangle + |11\rangle\right) \left(\alpha |0\rangle + \beta |1\rangle\right) \\
&+ \frac{1}{2\sqrt{2}} \left(|00\rangle - |11\rangle\right) \left(\alpha |0\rangle - \beta |1\rangle\right) \\
&+ \frac{1}{2\sqrt{2}} \left(|01\rangle + |10\rangle\right) \left(\alpha |1\rangle + \beta |0\rangle\right) \\
&+ \frac{1}{2\sqrt{2}} \left(|01\rangle - |10\rangle\right) \left(\alpha |1\rangle - \beta |0\rangle\right) \\
&= \frac{1}{2} \sum_{ab} |\beta_{ab}\rangle |\psi_{ab}\rangle .
\end{aligned}
$$

Alternatively, we may invert the definition of the Bell basis

$$
\begin{aligned}
|00\rangle &= \frac{1}{\sqrt{2}} \left(|\beta_{00}\rangle + |\beta_{10}\rangle\right), \\
|01\rangle &= \frac{1}{\sqrt{2}} \left(|\beta_{01}\rangle + |\beta_{11}\rangle\right), \\
|10\rangle &= \frac{1}{\sqrt{2}} \left(|\beta_{01}\rangle - |\beta_{11}\rangle\right), \\
|11\rangle &= \frac{1}{\sqrt{2}} \left(|\beta_{00}\rangle - |\beta_{10}\rangle\right);
\end{aligned}
$$

and use it on the expansion

$$
\begin{aligned}
|\psi\rangle |\Phi\rangle &= \frac{1}{\sqrt{2}} \left(\alpha |00\rangle |0\rangle + \alpha |01\rangle |1\rangle + \beta |10\rangle |0\rangle + \beta |11\rangle |1\rangle\right) \\
&= \frac{1}{2} \left[\alpha \left(|\beta_{00}\rangle + |\beta_{10}\rangle\right) |0\rangle + \alpha \left(|\beta_{01}\rangle + |\beta_{11}\rangle\right) |1\rangle \right. \\
&\left. + \beta \left(|\beta_{01}\rangle - |\beta_{11}\rangle\right) |0\rangle + \beta \left(|\beta_{00}\rangle - |\beta_{10}\rangle\right) |1\rangle\right] \\
&= \frac{1}{2} \sum_{ab} |\beta_{ab}\rangle |\psi_{ab}\rangle .
\end{aligned}
$$

Exercise 3 One can easily show that $\{|\psi_{00}\rangle, |\psi_{11}\rangle\}$ and $\{|\psi_{01}\rangle, |\psi_{10}\rangle\}$ each constitute an orthonormal basis of the two-dimensional Hilbert space. A balanced mixture of an orthonormal basis (a mixture of all elements of the basis with the same probability) yields in general the maximally mixed state $\frac{1}{d} Id$, with d the dimensionality of the Hilbert space. We can regard our case as the balanced mixture of two maximally mixed states, one coming from each orthonormal basis. The result is, therefore, the maximally mixed state.

As for the partial trace of a Bell state, explicit computation yields

$$\begin{aligned} Tr_A \left|\beta_{ab}\right\rangle \left\langle\beta_{ab}\right| &= \frac{1}{2} Tr_A \left(\left|0a\right\rangle + (-1)^b \left|1\bar{a}\right\rangle\right) \left(\left\langle 0a\right| + (-1)^b \left\langle 1\bar{a}\right|\right) \\ &= \frac{1}{2} \left\langle 0\right|_A \left(\left|0a\right\rangle + (-1)^b \left|1\bar{a}\right\rangle\right) \left(\left\langle 0a\right| + (-1)^b \left\langle 1\bar{a}\right|\right) \left|0\right\rangle_A \\ &+ \frac{1}{2} \left\langle 1\right|_A \left(\left|0a\right\rangle + (-1)^b \left|1\bar{a}\right\rangle\right) \left(\left\langle 0a\right| + (-1)^b \left\langle 1\bar{a}\right|\right) \left|1\right\rangle_A \\ &= \frac{1}{2} \left(\left|a\right\rangle \left\langle a\right| + \left|\bar{a}\right\rangle \left\langle \bar{a}\right|\right) = \frac{1}{2} Id. \end{aligned}$$

Exercise 5 Let us carefully label the states and follow the same procedure as in exercise 2

$$\left|\beta_{00}\right\rangle_{AC1} \left|\beta_{00}\right\rangle_{C2B} = \frac{1}{2} \left(\left|0\right\rangle_A \left|0\right\rangle_{C1} + \left|1\right\rangle_A \left|1\right\rangle_{C1}\right) \left(\left|0\right\rangle_{C2} \left|0\right\rangle_B + \left|1\right\rangle_{C2} \left|1\right\rangle_B\right)$$

$$\begin{aligned} &= \frac{2}{4} \left(\left|0\right\rangle_A \left|0\right\rangle_B \left|0\right\rangle_{C1} \left|0\right\rangle_{C2} + \left|1\right\rangle_A \left|0\right\rangle_B \left|1\right\rangle_{C1} \left|0\right\rangle_{C2} + \left|0\right\rangle_A \left|1\right\rangle_B \left|0\right\rangle_{C1} \left|1\right\rangle_{C2} + \left|1\right\rangle_A \left|1\right\rangle_B \left|1\right\rangle_{C1} \left|1\right\rangle_{C2}\right) \\ &+ \frac{1}{4} \left(\left|0\right\rangle_A \left|0\right\rangle_B \left|1\right\rangle_{C1} \left|1\right\rangle_{C2} + \left|1\right\rangle_A \left|0\right\rangle_B \left|0\right\rangle_{C1} \left|1\right\rangle_{C2} + \left|0\right\rangle_A \left|1\right\rangle_B \left|1\right\rangle_{C1} \left|0\right\rangle_{C2} + \left|1\right\rangle_A \left|1\right\rangle_B \left|0\right\rangle_{C1} \left|0\right\rangle_{C2}\right) \\ &- \frac{1}{4} \left(\left|0\right\rangle_A \left|0\right\rangle_B \left|1\right\rangle_{C1} \left|1\right\rangle_{C2} + \left|1\right\rangle_A \left|0\right\rangle_B \left|0\right\rangle_{C1} \left|1\right\rangle_{C2} + \left|0\right\rangle_A \left|1\right\rangle_B \left|1\right\rangle_{C1} \left|0\right\rangle_{C2} + \left|1\right\rangle_A \left|1\right\rangle_B \left|0\right\rangle_{C1} \left|0\right\rangle_{C2}\right) \end{aligned}$$

$$\begin{aligned} &= \frac{1}{4} \left(\left|00\right\rangle_{AB} + \left|11\right\rangle_{AB}\right) \left(\left|00\right\rangle_{C1C2} + \left|11\right\rangle_{C1C2}\right) \\ &+ \frac{1}{4} \left(\left|00\right\rangle_{AB} - \left|11\right\rangle_{AB}\right) \left(\left|00\right\rangle_{C1C2} - \left|11\right\rangle_{C1C2}\right) \\ &+ \frac{1}{4} \left(\left|01\right\rangle_{AB} + \left|10\right\rangle_{AB}\right) \left(\left|01\right\rangle_{C1C2} + \left|10\right\rangle_{C1C2}\right) \\ &+ \frac{1}{4} \left(\left|01\right\rangle_{AB} - \left|10\right\rangle_{AB}\right) \left(\left|01\right\rangle_{C1C2} - \left|10\right\rangle_{C1C2}\right) \\ &= \frac{1}{2} \sum_{ab} \left|\beta_{ab}\right\rangle_{AB} \left|\beta_{ab}\right\rangle_{C1C2}. \end{aligned}$$

As in the case of teleportation, a measurement by Carol on her qubit pair on the Bell basis will collapse Alice's and Bob's qubits in a Bell state. After Carol's broadcasting of the results, Alice and Bob will know exactly which Bell state they share.